ORIGINAL RESEARCH ARTICLE



PTN-PTPRZ signalling is involved in deer antler stem cell regulation during tissue regeneration

¹Faculty of Dentistry, Sir John Walsh Research Institute, University of Otago, Dunedin, New Zealand

²Institute of Antler Science and Product Technology, Changchun Sci-Tech University, Changchun, China

Correspondence

Dawn Coates, Faculty of Dentistry, University of Otago, Dunedin 9016, New Zealand. Email: dawn.coates@otago.ac.nz

Funding information

Velvet Antler Research New Zealand, Grant/Award Number: 2017150

Abstract

A growing deer antler contains a stem cell niche that can drive endochondral bone regeneration at up to 2 cm/day. Pleiotrophin (PTN), as a multifunctional growth factor, is found highly expressed at the messenger RNA level within the active antler stem cell tissues. This study aims to map the expression patterns of PTN protein and its receptors in a growing antler and investigate the effects of PTN on antler stem cells in vitro. Immunohistochemistry was employed to localise PTN/midkine (MDK) and their functional receptors, protein tyrosine phosphatase receptor type Z (PTPRZ), anaplastic lymphoma kinase (ALK), NOTCH2, and integrin $\alpha_V \beta_3$ on serial slides of the antler growth centre. PTN was found to be the dominantly expressed growth factor in the PTN/MDK family. High expression of PTPRZ and ALK colocalised with PTN was found suggesting a potential interaction. The high levels of PTN and PTPRZ reflected the antler stem cell activation status during the regenerative process. When antler stem cells were cultured in vitro under the normoxic condition, no PTN protein was detected and exogenous PTN did not induce differentiation or proliferation but rather stem cell maintenance. Collectively, the antler stem cell niche appears to upregulate PTN and PTPRZ in vivo, and PTN-PTPRZ signalling may be involved in regulating antler stem cell behaviour during rapid antler regeneration.

KEYWORDS

antler stem cell, hypoxia, proliferation and migration, PTN, regeneration

1 | INTRODUCTION

The ability to completely regenerate organs in adult mammals is unique (Seifert & Voss, 2013). The annual full regeneration of a deer antler makes it unique among mammals, and evidence, to date, indicates that this is a stem cell-based process (Wang et al., 2019). Antler regeneration occurs in yearly cycles involving growth, calcification, antler skin (velvet) shedding with retention of the bony antler and finally casting of the antler to allow the next year's growth to occur (Goss, 1983). Regeneration is initiated from a pool of dormant stem cells residing in the periosteum of the permanent bony extension on the deer skull, termed the pedicle (Li et al., 2007). Each

year, stem cells from the distal pedicle periosteum form an active growth centre (GC) from which an antler is regenerated. This active stem cell niche is responsible for the growth of the new antler at rates of up to 2 cm/day (Li, 2012). During the rapid growth phase, the antler tip consists of a number of distinct layers, which from distal to proximal region are as follows: skin, mesenchyme, precartilage (PC), cartilage, and bone infiltrated with blood vessels (Li et al., 2002). A high density of mesenchymal stem cells has been identified within the mesenchymal and PC layers (Dong et al., 2020). The deer antler is, therefore, an ideal regenerative model to investigate the factors involved in the development of an active stem cell niche and the processes of rapid cellular growth and differentiation.

Pleiotrophin (PTN) messenger RNA (mRNA) has been identified as being highly upregulated within the undifferentiated cells of the antler tip mesenchyme and the maturing chondroblasts of the PC region in the growing antler (Clark et al., 2006). PTN was first discovered as a neurite outgrowth-enhancing factor from young rat brains (Rauvala & Pihlaskari, 1987). The human, bovine, and rat PTN genes have sequences (Y. S. Li et al., 1990; Merenmies & Rauvala, 1990), which encode proteins of 168 amino acids. The interspecies conservation of amino acid sequences is remarkable and, to the best of authors' knowledge, the highest of any of the known cytokines (Hampton et al., 1992; Y. S. Li et al., 1992, 1990). PTN is capable of various functions including cell proliferation, survival, differentiation and migration, stem cell maintenance, and tumorigenesis (Himburg et al., 2012; Xu et al., 2014). Together with its family member midkine (MDK), they are heparin-binding growth factors (Muramatsu, 2014), have ca. 50% homology in their amino acid sequences and contain similar conserved C and N domains. Mouse models with either PTN or knocked out MDK genes exhibit similar moderate abnormalities (Kaplan et al., 2003; Sakurai et al., 2001); however, mice with simultaneously knocked out PTN and MDK genes display severe abnormalities (Herradon et al., 2005; Muramatsu et al., 2006; Sone et al., 2011; Zou et al., 2006); thus, suggesting that the functions of PTN and MDK are complementary.

PTN regulates multiple physiological and pathological processes by binding with diverse receptors (Xu et al., 2014). It has been identified as the most potent natural ligand for protein tyrosine phosphatase receptor type Z (PTPRZ) with strong inhibition of its phosphatase activity (Fukada et al., 2006; Meng et al., 2000). Anaplastic lymphoma kinase (ALK) receptor is a tyrosine kinase, which was regarded as an "orphan receptor" until it was found to be a substrate for PTPRZ and activated through the PTN/PTPRZ signalling axis (Deuel, 2013; Stoica et al., 2001). Notch receptor 2 (NOTCH2) is one of the four known Notch receptors in mammals (Fleming, 1998), which acts as a receptor for MDK under both physiological (Huang et al., 2008) and pathological (Kishida et al., 2013) conditions. No evidence supports a direct interaction between PTN and NOTCH2; however, PTN has an overlapping expression with NOTCH2 during ocular development (Cui & Lwigale, 2019), and it activates Notch signalling during haematopoietic stem cell expansion (Himburg et al., 2010). Integrin $\alpha_V \beta_3$ is comprised of integrin subunit alpha V (ITGAV) and integrin subunit beta 3 (ITGB3) (Hynes, 2002). It has been found to exclusively bind with PTN rather than MDK, and it functions as a receptor in PTN-induced endothelial cell migration, through PTPRZ (Mikelis et al., 2009).

A previous study has shown that the *PTN* gene is highly expressed in the deer antler tip and could have a putative role in angiogenesis and chondrogenesis (Clark et al., 2006). There is, however, no research investigating cervine PTN at the protein level. In this study, the cervine PTN protein was localised during different stages of antler regeneration. MDK, also a member of the PTN/MDK growth factor family, coupled with their main receptors was also localised on serial sections from the antler GC. The effects of exogenous PTN were investigated in vitro on antler-derived stem cells.

Identification and investigation of active factors from regenerating antlers may have significant impact on the field of regenerative medicine.

2 | MATERIALS AND METHODS

2.1 | Tissue collection and sample preparation

All tissues were collected from red deer (Cervus elaphus). Dormant pedicle periosteum (DPP; n = 3) and facial periosteum (FP; n = 3) were harvested for protein extraction from deer heads immediately after the slaughter in late summer (February in the southern hemisphere) at a local abattoir (Duncan New Zealand Venison). DPP (n = 3) tissues for the primary cell culture were harvested at the time of antler induction in late spring (November). Mid-beam antler periosteum (MAP) and GC (n = 3 each) tissues were obtained from commercially harvested velvet antler (~50-60 days of growth) at a deer research farm (AgResearch Invermay). GC sampling used methodology previously validated by Li et al. (2002), in which the reserve mesenchymal (RM) and PC layers of the GC were dissected for protein extraction and primary cell culture (Figure 1). DPP containing the dormant stem cells was collected as strips of periosteum from the proximal region of the pedicle for protein extraction and primary cell culture (Li & Suttie, 2003). MAP was collected as strips of mid-antler periosteum from antler at the time of commercial harvesting. FP was collected from the nasal bone periosteum, between the two eye sockets, and used as control tissue.

Tissues for morphology and immunohistochemistry were fixed in 10% neutral buffered formalin (LabServ) for 24 h and then transferred into phosphate-buffered saline (PBS; Gibco). Paraffin embedding of the tissues was conducted and 4μ m serial sections were obtained. The tissue for the primary cell culture was collected using sterile instruments after preparing the surrounding area with povidone-iodine Prep Pads and 70% alcohol cotton balls. Protein analysis tissues were snap-frozen in liquid nitrogen and stored at -80° C.

2.2 Masson's trichrome staining

After dewaxing and hydration of the antler tip tissues, Masson's trichrome staining was performed using the method reported by Bancroft and Stevens (1991). Sections were observed under an Eclipse TE2000 Inverted Microscope (Nikon) and images were captured by an Aperio Digital Slide Scanner (Leica Biosystems).

2.3 | Immunohistochemistry

Immunohistochemical detection for PTN, MDK, PTPRZ, ALK, NOTCH2, ITGAV, and ITGB3 was performed on 4- μ m serial sections of a paraffin-embedded antler tip tissue (Table S1).

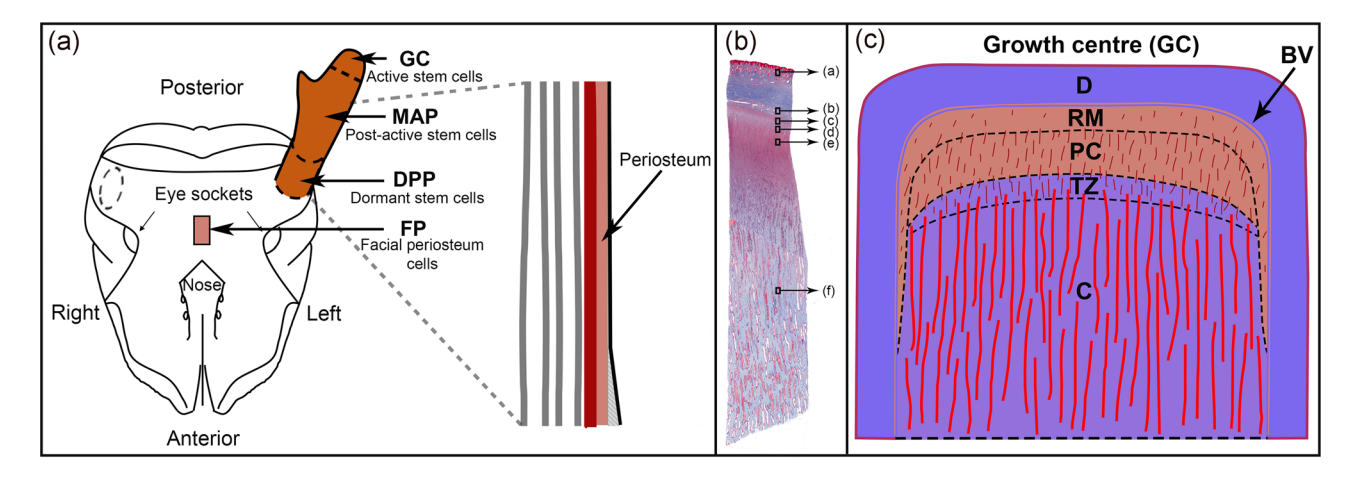


FIGURE 1 Deer antler stem cells during regeneration. (a) A schematic diagram of a deer antler. Facial periosteum (FP), dormant pedicle periosteum (DPP), mid-beam antler periosteum (MAP), and growth centre (GC). (b) Masson's trichrome staining of GC. Boxes indicate different layers as (a) dermis (D) with hair follicles; (b) across D, major blood vessels (BV) and reserve mesenchyme (RM); (c) RM; (d) RM and precartilage (PC); (e) PC; and (f) cartilage (C). (c) A schematic diagram of different tissue layers is derived from the Masson's trichrome staining of a growing antler tip. TZ, transition zone

Morphology was examined after haematoxylin and eosin staining. Immunohistochemistry for MDK, NOTCH2, ITGAV, and ITGB3 was conducted on sections dewaxed in xylene (3x) and then hydrated. Heat retrieval was performed with citrate buffer (0.01 M) at 95-100°C in a water bath. Slides were incubated for 30 min with 20% goat serum (Sigma-Aldrich) and 1% bovine serum albumin (BSA; Sigma-Aldrich)/PBS to block nonspecific binding sites and incubated at 4°C overnight using primary antibodies (Table S1) in a diluent of 5% goat serum + 1% BSA/PBS. Washing was followed by incubation in goat F(ab')2 anti-rabbit immunoglobulin G (IgG) H&L (Biotin) (5 µg/ml; Abcam) for 1 h and endogenous peroxidase blocking with 0.3% hydrogen peroxide (Sigma-Aldrich) in methanol. Detection was then performed using a Vectastain Elite ABC Strep Horseradish Peroxidase (HRP) Kit (Vector Laboratories), followed by a 3,3'-diaminobenzidine chromogen (Sigma-Aldrich). Immunohistochemistry for PTN, PTPRZ, and ALK was conducted using an automated BenchMark XT platform (Table S1; Ventana Medical Systems). Matched IgG controls were conducted on all tissues. Haematoxylin was used as the counterstain. Images were taken with an Aperio Digital Slide Scanner (Leica Biosystems) and analysed by Aperio ImageScope software (v12.3.2; Leica Biosystems).

2.4 Antler powder protein extraction

The antler powder was obtained from three manufacturers, produced by either a traditional method, freeze drying, or freeze drying after cryogenic processing. Two sets of 0.1-g samples (n = 3 per set) from each antler powder were suspended in 1-ml cold PBS with 1X EDTA-free protease inhibitor cocktail (Roche). One set was placed on an orbital shaker (100 rpm/min) for 2 h inside an ice box. A second set was sonicated on ice for 3×15 s with an amplitude of 50% using an ultrasonic homogeniser (Branson Ultrasonics).

The total protein content in the supernatants was collected and quantified using a DC protein assay (Bio-Rad).

2.5 | Enzyme-linked immunosorbent assay

PTN enzyme-linked immunosorbent assay (ELISA; catalog no. MBS455121; Mybiosource) was performed on the supernatants derived from the antler powder extractions as per the manufacturer's instruction. Results were normalised to the total protein content.

2.6 | Isolation and culture of antler stem cells

DPP strips containing the dormant stem cells (n = 3; Figure 1a) and the RM and PC layers of the GC, containing the active stem cells (n = 3; Figure 1b,c), were dissected and collected. After washing with sterile PBS, tissues were cut into fine pieces for subsequent explant culture in six-well plates (Thermo Fisher Scientific). The culture medium consisted of high-glucose Dulbecco's modified Eagle medium (DMEM) with 10% fetal bovine serum (FBS), 100-U/ml penicillin, 100-μg/ml streptomycin, 250-ng/ml amphotericin B, and 50-μg/ml gentamicin (All from Life Technologies), referred to hereafter as DMEM/10% FBS. Subsequent to the cells migrating out of the tissues but before reaching confluency, the media and tissue pieces were removed and attached cells were trypsinised for passaging. Dormant pedicle periosteum cells (DPPCs) and growth centre cells (GCCs) were then separately seeded into T25 culture flasks (Greiner Bio-One) and cultured at 37°C with 5% CO₂. After reaching 70% confluency, the cultured cells were cryopreserved with 90% FBS and 10% DMSO (Sigma-Aldrich) in liquid nitrogen for further use. All cells were used at P2 for subsequent experiments. Previous studies have

TABLE 1 The primer sequences for B2M, RPL40, and PTN

Gene	Primer
B2M (forward)	5'-GGCTGCTGTCGCTGTCT-3'
B2M (reverse)	5'-TCTGGTGGGTGTCTTGAGTAC-3'
RPL40 (forward)	5'-CGAGCCCAGTGACACCATT-3'
RPL40 (reverse)	5'-CGCAGACGAAGCACCAAGT-3'
PTN (forward)	5'-AGCAGTTTGGAGCGGAGTG-3'
PTN (reverse)	5'-TGGTCTTCAGAGCCGTGTTC-3'

confirmed that these cells retain their stemness (Li et al., 2009; Wang et al., 2018, 2019).

2.7 | Quantitation of osteogenesis

For osteogenic differentiation and quantitation, DPPCs and GCCs were seeded into 24-well plates (Greiner Bio-One) at a cell density of 6000 cells/cm². The next day (Day 0), the medium was changed to either the normal medium (DMEM/10% FBS; as above) or osteogenic medium containing DMEM/10% FBS with the addition of 100- μ M $_{L}$ -ascorbic acid 2-phosphate (Sigma-Aldrich), 10-nM dexamethasone (Sigma-Aldrich), and 5-mM β -glycerophosphate (Sigma-Aldrich). Normal and osteogenic media were changed every 48 h. After 7, 14, and 21 days, cells were fixed with 70% ice-cold ethanol. Osteogenic mineralisation was determined using an Osteogenesis Quantitation Kit (Merck). Cell images, after Alizarin Red S (ARS) staining, were captured using an Eclipse TE2000 Inverted Microscope (Nikon).

2.8 | Osteogenesis as determined by alkaline phosphatase production

The quantitative analysis of alkaline phosphatase (ALP) activity was conducted on GCCs seeded into 48-well plates (Greiner Bio-One) at a cell density of $3\times10^4\,\mathrm{cells/cm^2}$. The next day (Day 0), media were changed to DMEM/10% FBS with 100-ng/ml BMP-2 (PeproTech) to induce osteogenesis, as recently demonstrated by Ker et al. (2018). Recombinant human PTN (rhPTN; catalog no. 252-PL; R&D Systems) was added at physiological doses of 1, 10^2 , 10^4 , or $10^5\,\mathrm{pg/ml}$ and compared with carrier-only controls. The medium was changed every 48 h with the addition of fresh growth factors. After 6 days, cells were trypsinised (Life Technologies) and collected. The ALP activity (Abcam) was detected as per the manufacturer's instructions.

2.9 | Cell proliferation

GCCs were seeded into 96-well plates (Thermo Fisher Scientific) at the cell density of 6000 cells/cm². The next day (Day 0), two different media formulations were applied: one was DMEM high glucose plus 1% FBS, 100-U/ml penicillin, 100-µg/ml streptomycin, 250-ng/ml amphotericin B, 50-µg/ml gentamicin, and rhPTN at 0, 1, 10, 10^2 , 10^3 , 10^4 , 5×10^4 , or 10^5 pg/ml, and the other one was DMEM high glucose plus 10% FBS, 100-U/ml penicillin, 100-µg/ml streptomycin, 250-ng/ml amphotericin B, 50-µg/ml gentamicin, and 5×10^4 pg/ml rhPTN. PrestoBlue cell viability reagent (Thermo Fisher Scientific) was added 4 h before every medium change and incubated at 37° C with 5% CO $_2$. At 24, 48, 72, and 96 h, fluorescence was read with an excitation/emission wavelength of 560/590 nm using a Synergy 2 Multi-Mode Microplate Reader (BioTek).

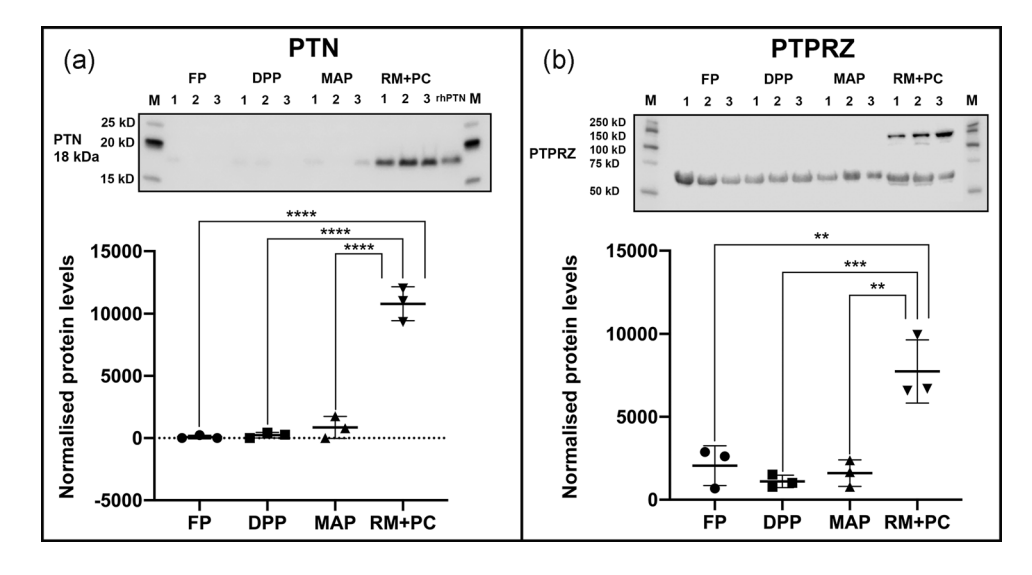


FIGURE 2 Stain-free western blotting to investigate the expression levels of pleiotrophin (PTN) (a) and protein tyrosine phosphatase receptor type Z (PTPRZ) (b) in the four tissue groups. Total protein loading was used for normalisation between samples. Normalised protein abundance is presented as the mean value \pm standard deviation. One-way analysis of variance with post hoc Tukey honestly significant difference test was performed. Fifty nanograms recombinant human PTN was used as a positive control. Due to anti-PTPRZ (b) being incubated after the stripping of anti-PTN (a), they shared the same marker (M) panels. DPP, dormant pedicle periosteum; FP, facial periosteum; MAP, mid-beam antler periosteum; RM + PC, reserve mesenchymal and precartilage layers in the growth centre. **p < .01, ***p < .001, ****p < .001.

2.10 | F-actin staining

After removing the media in the cell viability assay at 96 h, F-actin staining of GCCs under different PTN concentrations was performed. Cells were fixed in 10% neutral buffered formalin for 15 min and incubated with Alexa Fluor 647 Phalloidin (Thermo Fisher Scientific) for 45 min in the dark. 4′,6-Diamidino-2-phenylindole (DAPI; Thermo Fisher Scientific) was used as a nuclear counterstain. Fluorescence images were acquired using an EVOS M5000 Cell Imaging System (Thermo Fisher Scientific) equipped with Cy5 and DAPI light cubes for Alexa Fluor 647 phalloidin and DAPI staining, respectively.

2.11 | Sequence alignment

BLAST Needleman-Wunsch Global Alignment in NCBI (Altschul et al., 1997) was performed to compare human and red deer PTN and MDK

sequences. The amino acid sequences of human PTN (Accession No. P21246) and MDK (Accession No. P21741) were obtained from the UniProt database. The sequence for deer PTN was translated from the corresponding transcript sequence (Clark et al., 2006) and MDK (Accession No. OWK18060.1) obtained from the NCBI GenBank.

2.12 | Stain-free western blot

The western blot analysis for PTN and PTPRZ was conducted on the four tissue groups. Tissue lysate (9 μ l) from RM and PC layers of the GC, MAP, DPP, and FP (n=3 per group) were mixed with 3 μ l of 4X Laemmli loading buffer (Bio-Rad). rhPTN (50 ng) was used as a positive control. After heat denaturation, all samples were loaded into "Any kD Mini-PROTEAN TGX Stain-Free Protein Gels" (Bio-Rad) along with Precision Plus Protein WesternC protein standards (Bio-Rad). After running the sodium dodecyl sulfate (SDS)-polyacrylamide gel electrophoresis, proteins were detected with UV activation and imaged using

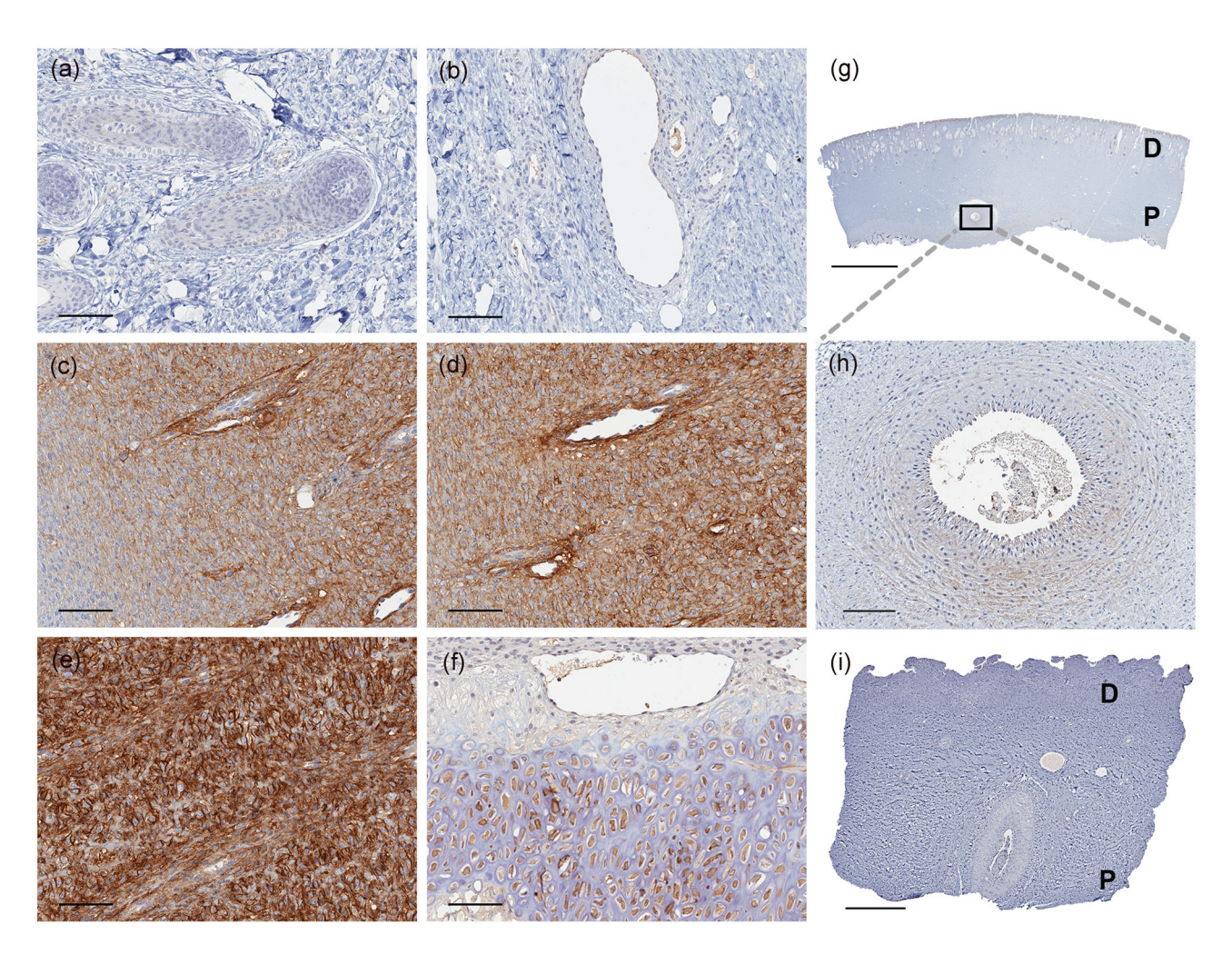


FIGURE 3 Representative immunohistochemical images of pleiotrophin (PTN) localisation (brown) in deer antler (n = 3). The images are from the distal (a) to the proximal (f) region of the antler tip, as indicated in Figure 1b. (a) Dermis with hair follicles; (b) across dermis, major blood vessels, and reserve mesenchyme; (c) reserve mesenchyme; (d) reserve mesenchyme and precartilage; and (e) precartilage and (f) cartilage. (g, h) PTN expression in mid-beam antler periosteum. (i) PTN in dormant pedicle periosteum. Haematoxylin was used as a counterstain. (a-f, h) Scale bar = $100 \,\mu\text{m}$; (g) scale bar = $2 \,\text{mm}$; (i) scale bar = $400 \,\mu\text{m}$. D, dermis and epidermal region; P, periosteum next to bone

a Gel Doc XR+ Imaging System (Bio-Rad) with Image Lab software (v5.2.1; Bio-Rad). The proteins were then transferred on Immun-Blot Low-Fluorescence polyvinylidene difluoride (PVDF) membranes (Bio-Rad) and imaged in a Gel Doc XR+ Imaging System (Bio-Rad) to assess transfer efficiency. Anti-PTN (0.4 µg/ml; catalog no. SC74443) was incubated at 4°C overnight. Secondary anti-mouse IgG HRP-conjugated antibody (Abcam) was used at 1:5000 dilution. Chemiluminescence imaging of the WesternC Blotting Standards was conducted with the addition of $1\,\mu l$ of StrepTactin-HRP conjugate (Bio-Rad) to every 10 ml of secondary antibody solution. Blots were developed using Clarity Western ECL substrate (Bio-Rad). Images were captured with an Odyssey Fc Imaging System (LI-COR) and Image Studio software (v5.2; LI-COR). The images were analysed and quantified in ImageJ (v1.52q; National Institutes of Health). The intensity of total protein within each lane was used for sample normalisation. After the detection for anti-PTN, the PVDF membrane was stripped with a buffer containing 62.5-mM Tris (pH 6.8, Thermo Fisher Scientific), 2% SDS (Thermo Fisher Scientific), and 100-mM β-mercaptoethanol (Sigma-Aldrich) at 50°C for 40 min. Anti-PTPRZ (0.8 µg/ml; catalog no. MBS2034104; Mybiosource) was incubated at 4°C overnight, followed by a secondary anti-rabbit IgG HRPconjugated antibody (Sigma-Aldrich) at 1:20,000 dilution.

PTN detection in the antler powders derived from different drying technologies was conducted on the extracts obtained from either stirring for 2 h or sonication at an amplitude of 50% for 3×15 s, both in ice. Extracts were ultrafiltered with Amicon Ultra-0.5 centrifugal filter devices (3 kDa; Millipore) to obtain 10 times concentrated samples. rhPTN (50 ng) and tissue lysate from RM and PC layers of the GC were used as positive controls.

For PTN and PTPRZ detection in DPPCs and GCCs, the supernatant was collected from cells cultured in normal and osteogenic media at 7 and 21 days, using the medium defined in Section 2.7. Cell lysates were extracted using M-PER mammalian protein extraction reagent (Thermo Fisher Scientific). rhPTN (50 ng) and tissue lysates from RM and PC layers of the GC were used as positive controls.

2.13 | Quantitative real-time polymerase chain reaction analysis of cellular hypoxia treatment

GCCs (n = 3) were seeded into T25 flasks and cultured until confluency reached 80%. The medium was then changed to either nonosteogenic medium, with reduced serum (DMEM/2% FBS), containing 100-U/ml penicillin, 100- μ g/ml streptomycin, 250- μ g/ml

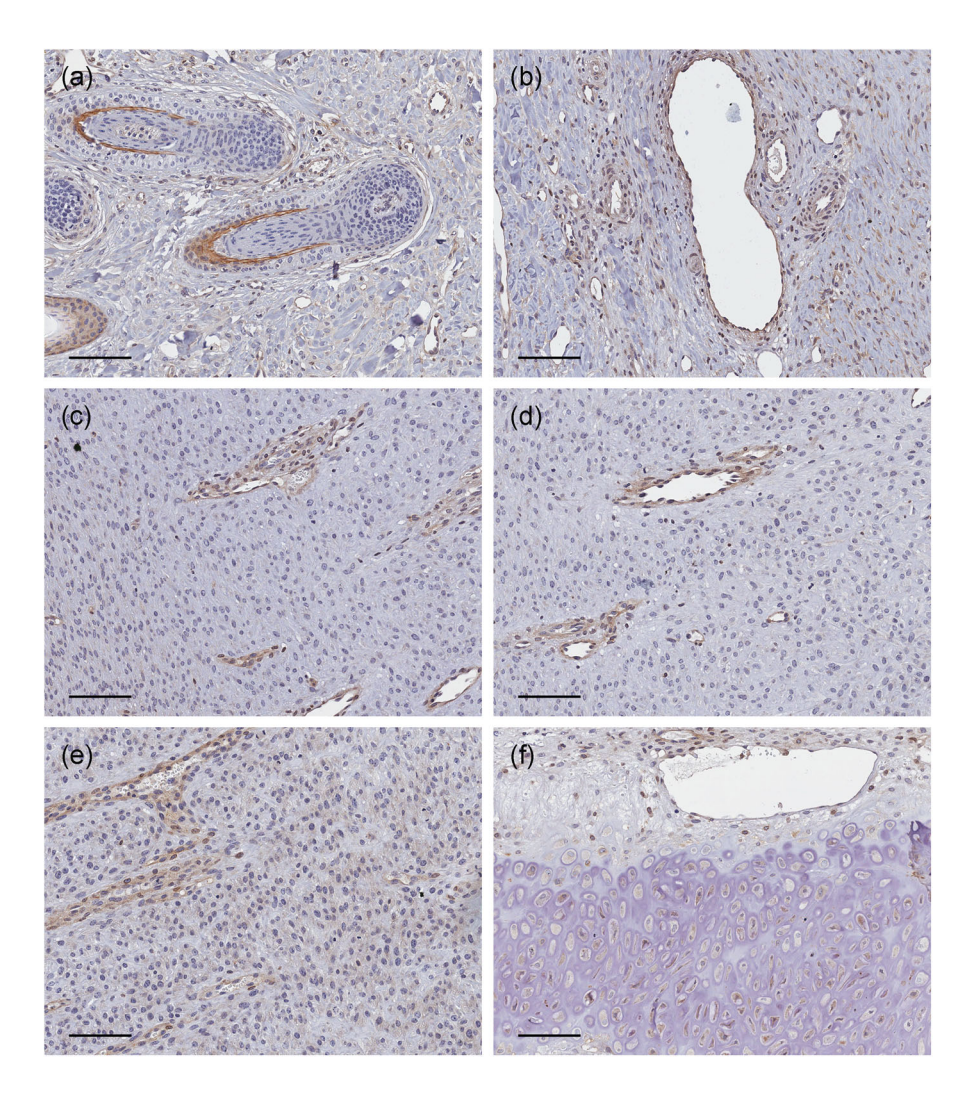


FIGURE 4 Representative immunohistochemical images of midkine localisation (brown) in deer antler (*n* = 3). The images are from the distal (a) to the proximal (f) region of the antler tip, as indicated in Figure 1b. (a) Dermis with hair follicles; (b) across dermis, major blood vessels, and reserve mesenchyme; (c) reserve mesenchyme and precartilage; (e) precartilage; and (f) cartilage. Haematoxylin was used as a counterstain. Scale bar = 100 µm

amphotericin B, and 50-µg/ml gentamicin or osteogenic medium (with reduced serum) containing nonosteogenic medium with the addition of 100-µM $\iota\text{-ascorbic}$ acid 2-phosphate, 10-nM dexamethasone, and 5-mM $\beta\text{-glycerophosphate}$. After 3 days, one set of cells in nonosteogenic or osteogenic media was cultured at 37°C with 5% CO₂, whereas the second set was cultured at 37°C with 5% CO₂/1% oxygen. Both sets were cultured for 24 h in normoxic or hypoxic conditions. A tissue from the antler GC PC layer was used as a positive control.

Total RNA was extracted from each sample using TRIzol (Thermo Fisher Scientific) and purified using a PureLink RNA Mini Kit (Thermo Fisher Scientific) according to the manufacturer's instructions. On-column PureLink DNase treatment (Thermo Fisher Scientific) was performed. Total RNA was stored at -80°C. Each sample was reverse-transcribed using 800 ng of total RNA using a Complementary DNA Reverse Transcription Kit (Thermo Fisher Scientific). Real-time polymerase chain reaction (RT-PCR) was then carried out on the QuantStudio 6 Flex Systems (Applied Biosystems) by using RT² SYBR Green ROX qPCR Mastermix (QIAGEN) according to the instructions. *Beta-2-microglobulin* (Table 1) and *ubiquitin A-52 residue ribosomal protein fusion product* 1 (Table 1) were chosen by NormFinder as the housekeeping genes; each sample was analysed in

duplicate. The $2^{-\Delta C_q}$ method was used to estimate the relative expression level of *PTN* mRNA (Table 1).

2.14 | Statistical analysis

The quantitative data were presented as the mean \pm standard deviation. One-sample t test and unpaired t test were performed to compare the data between two groups, and one-way analysis of variance with post hoc Tukey honestly significant difference test was performed to compare the data among multiple groups. All statistical analyses were carried out by GraphPad Prism (v8.2.1). A p-value of less than .05 was considered statistically significant.

3 | RESULTS

3.1 | PTN protein was more highly expressed than MDK during antler regeneration in vivo

Stain-free western blot analysis and immunohistochemistry were performed to investigate PTN expression levels during antler

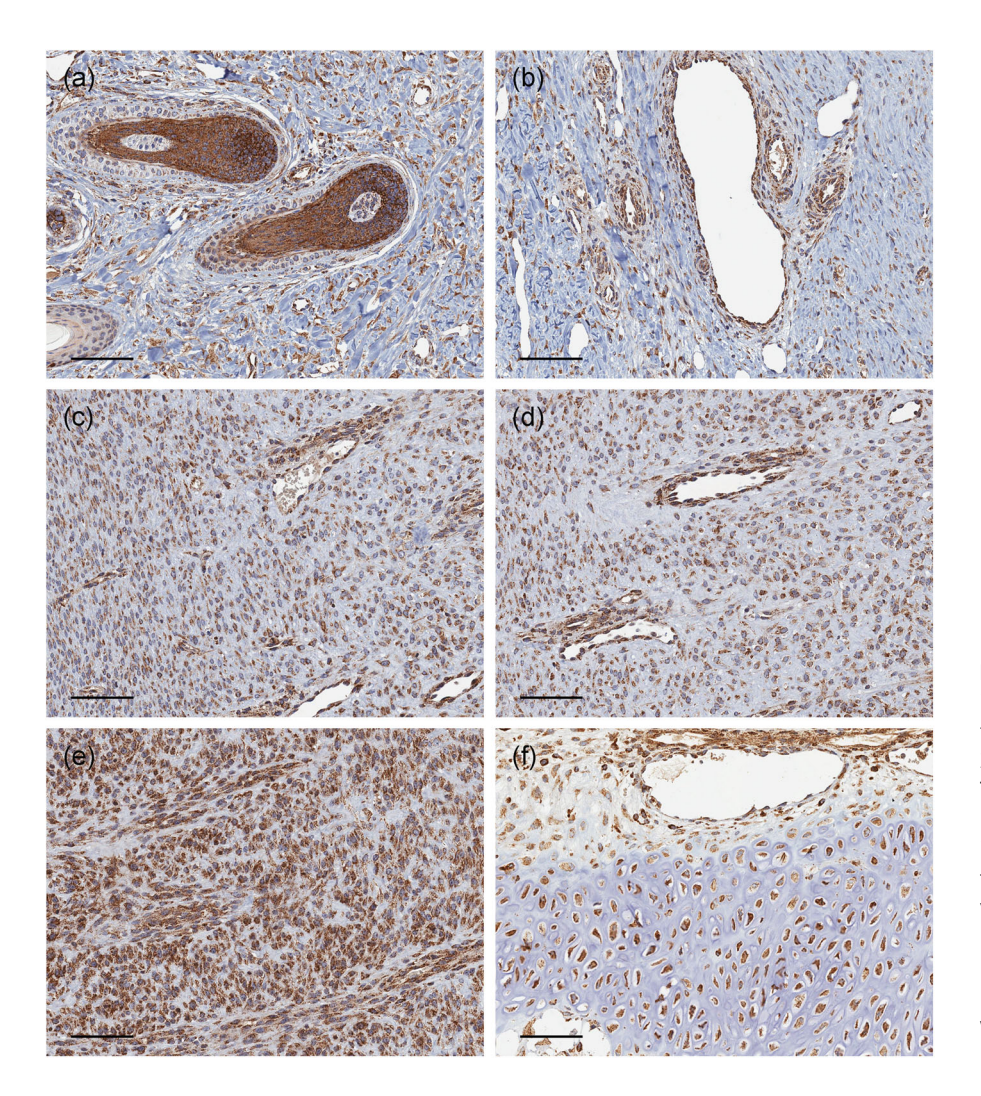
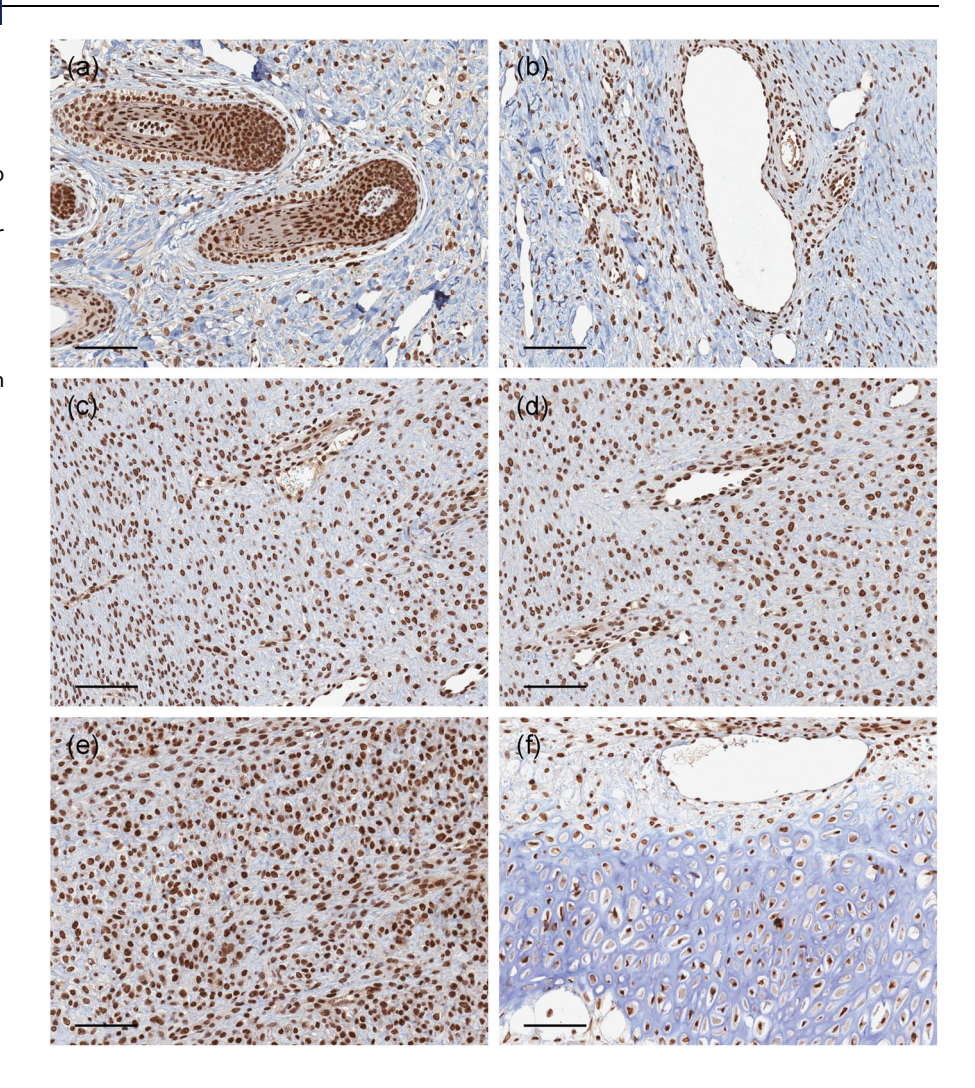


FIGURE 5 Representative immunohistochemical images of protein tyrosine phosphatase receptor type Z localisation (brown) in deer antler (*n* = 3). The images are from the distal (a) to the proximal (f) region of the antler tip, as indicated in Figure 1b. (a) Dermis with hair follicles; (b) across dermis, major blood vessels, and reserve mesenchyme; (c) reserve mesenchyme; (d) reserve mesenchyme and precartilage; (e) precartilage; and (f) cartilage. Haematoxylin was used as a counterstain. Scale bar = 100 μm

FIGURE 6 Representative immunohistochemical images of anaplastic lymphoma kinase (ALK) receptor tyrosine kinase localisation (brown) in deer antler (n = 3). The images are from the distal (a) to the proximal (f) region of the antler tip, as indicated in Figure 1b. (a) Dermis with hair follicles; (b) across dermis, major blood vessels, and reserve mesenchyme; (c) reserve mesenchyme; (d) reserve mesenchyme and precartilage; (e) precartilage; and (f) cartilage. Haematoxylin was used as a counterstain. Scale bar = $100 \mu m$



regeneration. PTN was found in high levels within the active stem cell layers of the GC during rapid regeneration; it was hardly detectable in tissues from other stages (Figures 2a and 3). When investigated by immunohistochemistry, PTN was highly expressed in the RM and PC layers of the GC with only light staining in the dermal endothelial cells and mature chondrocytes of the cartilage layer (Figures 3a-f and S2). The amino acid sequence alignment between deer PTN and MDK showed homology (43% identity) similar to the comparison between human PTN and MDK (42% identity) (Figures S1a and S1c and Table S2). Dot matrix plots of both comparisons further confirmed the sequence conservation between human and deer (Figures S1b and S1d). Immunohistochemistry for MDK, the other member of the PTN/ MDK family, was performed. MDK was mainly associated with blood vessels within the GC layers (Figures 4 and S2). Within the dermal and blood vessel layers, positive cells were associated with hair follicles and major blood vessels (Figure 4a,b); this contrasted with PTN immunohistochemistry, which was largely negative in these regions (Figure 3a,b).

3.2 | PTPRZ and ALK found to be highly expressed receptors for PTN/MDK in the antler GC

Immunohistochemical localisation of the PTN/MDK receptors PTPRZ and ALK was conducted on serial sections. PTPRZ and ALK were co-expressed with an intense positive signal throughout the GC from the dermis to cartilage layers (Figures 5, 6, and S2). The coexpression was particularly obvious in hair follicles and pericytes around blood vessels. ALK was only detected within the cell nucleus. Immunohistochemistry for NOTCH2 detected low-level expression, mainly in association with hair follicles (Figure 7a) and the hypertrophic chondroblasts of the cartilage zone (Figure 7f). ITGAV and ITGB3 immunohistochemistry detected fewer areas with positive signal when compared with the other receptors (Figures 8 and 9). Positive staining was associated with the hair follicles and around blood vessels. Low power imaging revealed that in the dermal and blood vessel layers, MDK displayed a similar expression pattern to PTPRZ and ALK (Figure S2). In all other layers, PTN had a very similar positive localisation pattern to PTPRZ and ALK (Figure S2).

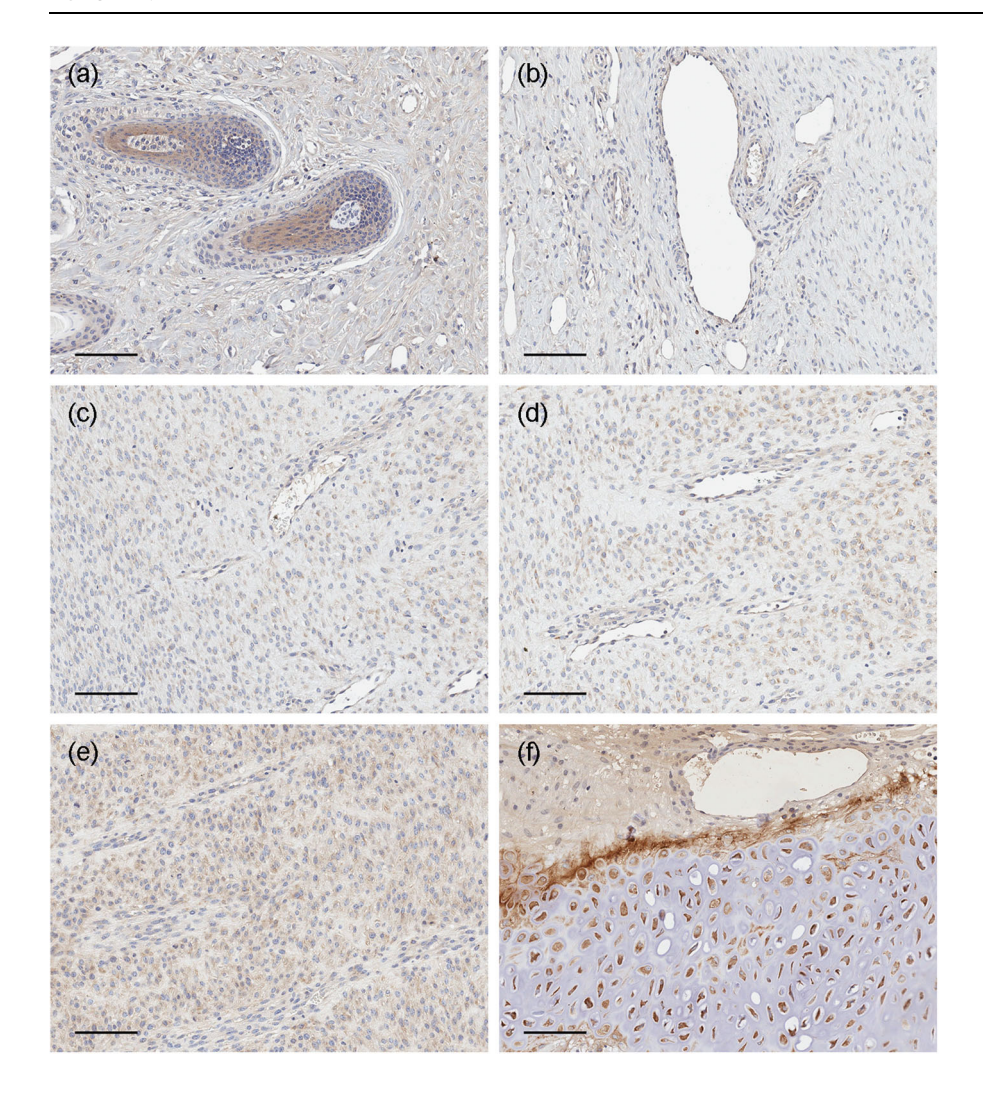


FIGURE 7 Representative immunohistochemical images of Notch receptor 2 localisation (brown) in the deer antler (n = 3). The images are from the distal (a) to the proximal (f) region of the antler tip, as indicated in Figure 1b. (a) Dermis with hair follicles; (b) across dermis, major blood vessels, and reserve mesenchyme; (c) reserve mesenchyme; (d) reserve mesenchyme and precartilage; (e) precartilage; and (f) cartilage. Haematoxylin was used as a counterstain. Scale bar = $100 \, \mu m$

3.3 | PTPRZ co-localised with PTN during antler stem cell activation

As the main receptor for PTN, expression levels of PTPRZ, together with PTN, were examined in different antler regeneration stages (Figure 2). Both PTN and PTPRZ had the highest expression levels in the RM/PC layers, in which the active antler stem cells reside (Dong et al., 2020). The quantitative analysis showed that the expression levels of PTN and PTPRZ were significantly lower (p < .01) in the nonactive antler stem cell tissues including MAP (post-active stem cells), DPP (dormant stem cells), and control FP cells when compared with the mesenchymal/PC layers. Western blot results, thus, indicated that PTN and PTPRZ levels were positively correlating to the antler stem cell activation status.

3.4 | PTN protein detected in antler powder extracts

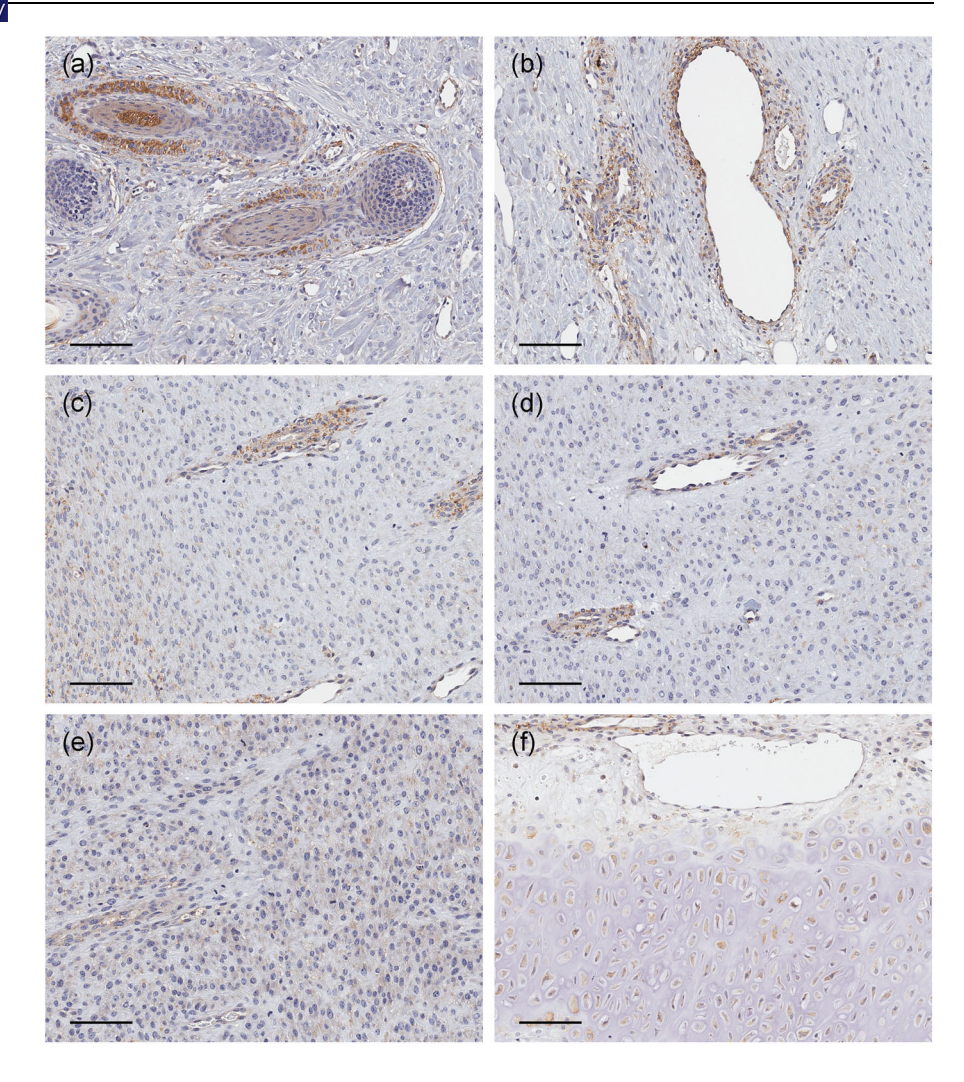
The presence of PTN protein in the whole stick antler, commercially harvested during the rapid regeneration period (50–60 days of growth), was further determined. The PTN concentration, as

determined by ELISA, was normalised using the levels of extracted protein from antler powders with different processing methods (Figure 10a). Freeze-dried antler powders contained the highest level of PTN as a proportion of total protein. The mean PTN concentration in samples extracted using sonication was nearly twice to that obtained from buffer extraction. The western blot analysis confirmed the presence of one band consistent at the correct molecular weight in both sonicated and buffer-extracted freeze-dried antler powder (Figure 10b). These results, thus, indicate a processing/extraction method to obtain PTN from the whole antler sticks and that PTN may be one of the important growth factors found not only within the GC but also in the whole stick antler.

3.5 | Osteogenesis of antler stem cells

Osteogenic differentiation of antler stem cells cultured from DPPCs (Figure 11a) and GCCs (Figure 11b) cells was evaluated by ARS staining. Both DPPCs and GCCs formed bone nodules under osteogenic medium rather than the normal medium. There was an increase in cellular mineralisation in osteogenic medium as compared with the normal medium; however, a larger variance in calcium

FIGURE 8 Representative immunohistochemical images of integrin subunit alpha V localisation (brown) in deer antler (n = 3). The images are from the distal (a) to the proximal (f) region of the antler tip, as indicated in Figure 1b. (a) Dermis with hair follicles; (b) across dermis, major blood vessels, and reserve mesenchyme; (c) reserve mesenchyme; (d) reserve mesenchyme and precartilage; (e) precartilage; and (f) cartilage. Haematoxylin was used as a counterstain. Scale bar = $100 \mu m$



production was observed in the osteogenic medium. Interestingly, the mean values of ARS concentration under the normal medium from either DPPCs or GCCs were quite close between 7, 14, and 21 days.

3.6 | Effect of PTN on the proliferation and osteogenesis of active antler stem cells in vitro

To investigate the effect of PTN on antler stem cells in vitro, PTN expression levels in cell culture supernatants and lysates were firstly investigated using western blot. No PTN protein was detected in either DPPCs/GCCs supernatants or their lysates (Figure 12a,b). DPPCs and GCCs cell lysates were also investigated for the presence of the PTPRZ receptor. Only low-level expression was detected as compared with the active stem cell tissues (Figure 12b). The amino acid sequence alignment revealed a high similarity between human and deer PTN, with an identity score of 96% (Figure S1e,f; Table S2). The effects of rhPTN on osteogenesis and proliferation of the active antler stem cells (GCCs) were further evaluated.

To investigate the effects of rhPTN on the osteogenic differentiation of GCCs, the relative levels of ALP were measured after 6 days of treatment (Figure 12c). Four concentrations of rhPTN were

investigated and ALPs levels were not significantly different from the control cells without rhPTN. Proliferation assays were also conducted on the GCCs cultured in 1% FBS using seven different rhPTN concentrations. A significant reduction in proliferation was detected as early as 24 h (p = .0016; Figure 12d) and 48 h (p = .0015; Figure 12d). A biphasic effect on proliferation was found, in which low and high doses of rhPTN reduced proliferation, whereas 1 ng/ml of rhPTN had no significant effect. F-actin staining of the GCCs at 96 h indicated no evidence of nodule formation or morphological differences in the cells cultured in rhPTN (Figure 12e). F-actin staining of GCCs cultured in 1% or 10% FBS with 5×10^4 pg/ml rhPTN displayed a similar morphology, suggesting that low FBS content in the media did not cause differentiation of the GCCs.

3.7 | PTN expression level under hypoxia

To investigate the effect of hypoxia on *PTN* expression by GCCs, the relative level of *PTN* was detected by quantitative reverse-transcriptase RT-PCR (Figure 13). GCCs cultured in nonosteogenic and osteogenic media under normoxia or hypoxia were collected. A mild, but significant, induction of *PTN* expression was found under hypoxia as compared with

11

FIGURE 9 Representative immunohistochemical images of integrin subunit beta 3 localisation (brown) in deer antler (*n* = 3). The images are from the distal (a) to the proximal (f) region of the antler tip, as indicated in Figure 1b. (a) Dermis with hair follicles; (b) across dermis, major blood vessels, and reserve mesenchyme; (c) reserve mesenchyme; (d) reserve mesenchyme and precartilage; (e) precartilage; and (f) cartilage. Haematoxylin was used as a counterstain. Scale bar = 100 μm

normoxia in both kinds of culture media; the difference was more evident in the nonosteogenic as compared with osteogenic media.

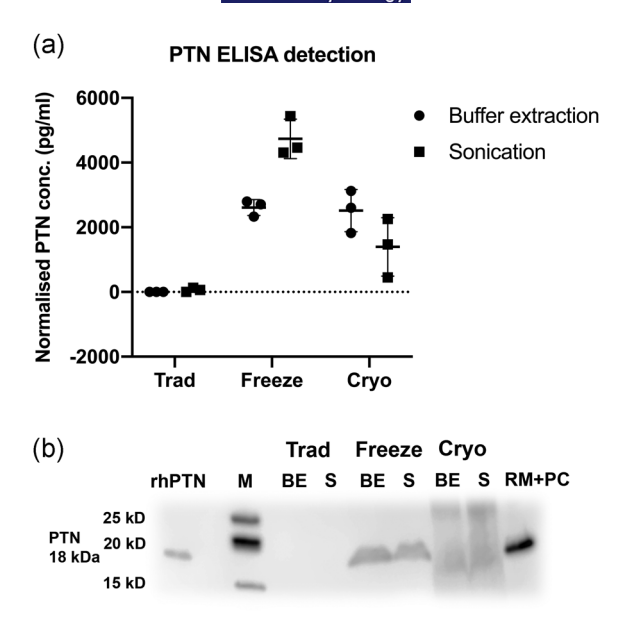
4 | DISCUSSION

A deer antler is a unique model of mammalian organ regeneration in which activated stem cells drive rapid endochondral bone growth in a controlled manner. The antler has been shown to differentially express PTN mRNA in a suppression subtraction hybridisation library, with the PTN transcript also highly expressed by in situ hybridisation within the active stem cell centre of the growing antler tip (Clark et al., 2006). This makes PTN potentially a key regulator involved in antler regeneration. In the current study, the expression of PTN protein was investigated in different antler regeneration stages including the whole stick of growing antler, all layers within the antler tip GC, post-active stem cells in the MAP, dormant stem cells in the pedicle periosteum, and control FP cells. The research also further investigated the functions of PTN in antler growth in vivo and antler stem cells in vitro. PTN was identified as the most highly expressed growth factor, of the PTN/MDK family, within the antler GC. Detection for PTN in different antler tissues revealed its

dominant expression in tissues associated with rapid antler regeneration, rather than dormant stem cell niches. The results, therefore, confirmed that PTN may be a critical growth factor participating in the regulation of rapid antler regeneration in vivo.

PTN's functions were investigated by detecting its potential receptors on serial sections of GC tissues. As a member of the receptor-type protein tyrosine phosphatase family (Levy et al., 1993), PTPRZ's phosphatase activity can be inactivated by the binding of either PTN or MDK (Fukada et al., 2006; Kadomatsu et al., 2013). The inactivation of phosphatase activity causes an increase of tyrosine phosphorylation in the substrates of PTPRZ, with influences on multiple physiological and pathological processes, such as angiogenesis, osteogenesis, and tumorigenesis (Lamprou et al., 2014; Papadimitriou et al., 2016). The expression of PTPRZ is specifically upregulated by hypoxia-inducible factor 2α (HIF- 2α) but not 1α , in both normal and tumour cell lines (V. Wang et al., 2005, 2010). In the current study, the expression of MDK in the dermal and blood vessel layers, as well as PTN in the other layers of the GC, showed colocalisation with PTPRZ immunohistochemistry, suggesting that PTPRZ could act as their receptor during rapid antler regeneration.

ALK, as a downstream tyrosine kinase, is activated as a result of ligand-induced dimerisation of the D1 domain in PTPRZ, an action



PTN concentration as detected by ELISA. Antler powders were obtained from traditional (Trad), freeze drying (Freeze), and cryogenic/freeze-drying (Cryo) methods. Total protein was obtained by buffer extraction (BE) or sonication (S), and used for normalisation. The normalised PTN concentration is presented as the mean value ± standard deviation. (b) PTN abundance as detected by western blot. Tissue lysate from reserve mesenchymal and precartilage layers (RM+PC) in the growth centre and 50-ng recombinant human PTN (rhPTN) were used as positive controls. ELISA, enzyme-linked immunosorbent assay; M, marker

most commonly attributed to PTN as well as MDK binding (Deuel, 2013; Xia et al., 2019). The activated ALK is ligand-dependent and involved in numerous biological processes, such as nerve development and tissue repair (Wellstein, 2012). ALK is mainly found in the cytoplasm as well as in the nucleus when fused with nucleophosmin (NPM) (Minoo & Wang, 2012). NPM provides a nuclear localisation domain and results in increased trafficking of ALK to the nucleus (Bischof et al., 1997). The fusion of NPM-ALK deregulates the kinase activity of ALK and induces a series of physiological and pathological processes including proliferation and tumorigenesis (Chiarle et al., 2008). This study found co-expression of PTPRZ with nuclear expression of ALK, indicating the tyrosine phosphorylation of ALK and its subsequent chaperoning to the nucleus via NPM. NPM was also recently reported to be highly expressed in active antler stem cells (Dong et al., 2020). Thus, NPM-ALK fusion in the nucleus could contribute as a rate-limiting proliferative step for stem cells during endochondral bone formation and not just for glioblastoma cells, as has been previously reported (Powers et al., 2002).

Our results showed that the MDK-PTPRZ-ALK signalling axis may be involved in angiogenesis, based on their co-expression around blood vessels (Choudhuri et al., 1997). The expression profile of PTN within the GC suggests that the PTN-PTPRZ-ALK signalling axis may participate in multiple processes including neurogenesis (Perez-Pinera et al., 2007), chondrogenesis (Bouderlique et al., 2014) and regulation of the stem cell niche (Himburg et al., 2012, 2014). Specific substrate activation of PTPRZ may, thus, be the key to bridge upstream PTN/MDK dimerisation and phosphatase

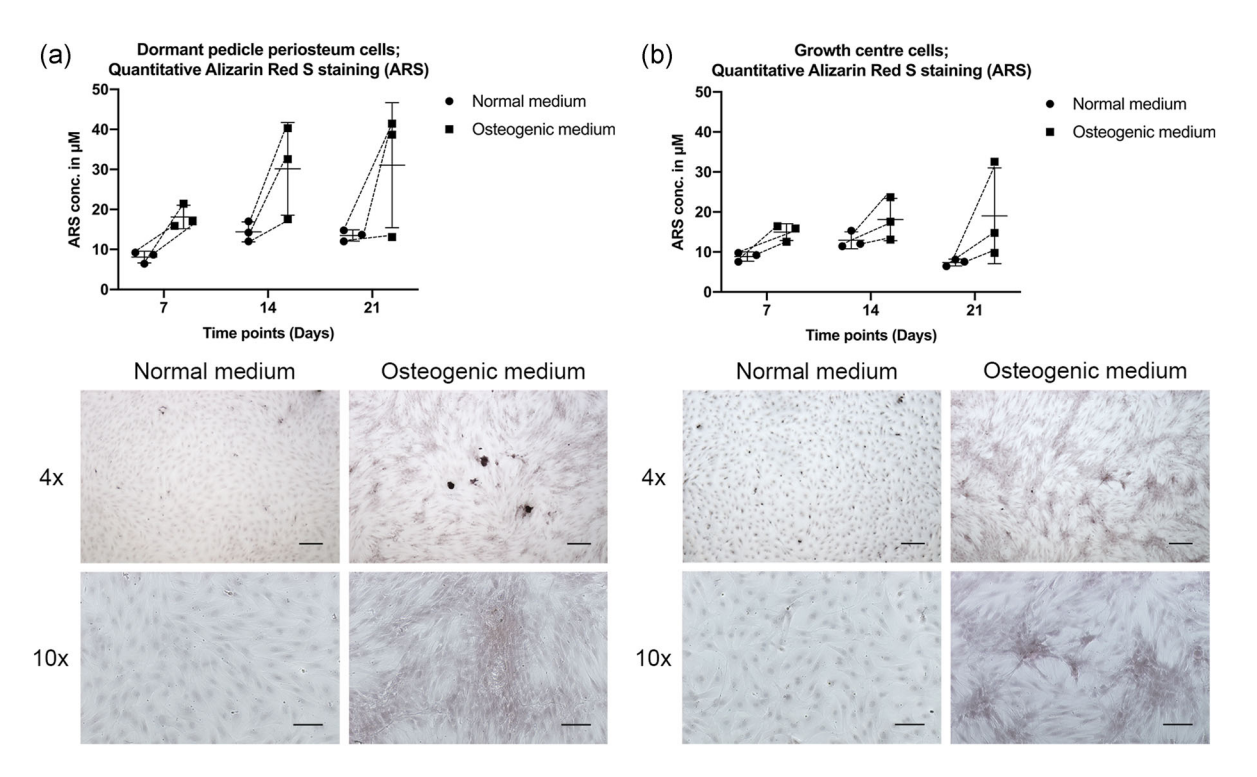


FIGURE 11 Alizarin Red S (ARS) staining of dormant pedicle periosteum cells (DPPCs) and growth centre cells (GCCs). (a) DPPCs and (b) GCCs under normal and osteogenic media were stained with ARS at 7, 14, and 21 days. The ARS concentration is presented as the mean value \pm standard deviation. Cell images were taken at 21 days after ARS staining. Scale bar (×4) = 200 μ m; scale bar (×10) = 100 μ m

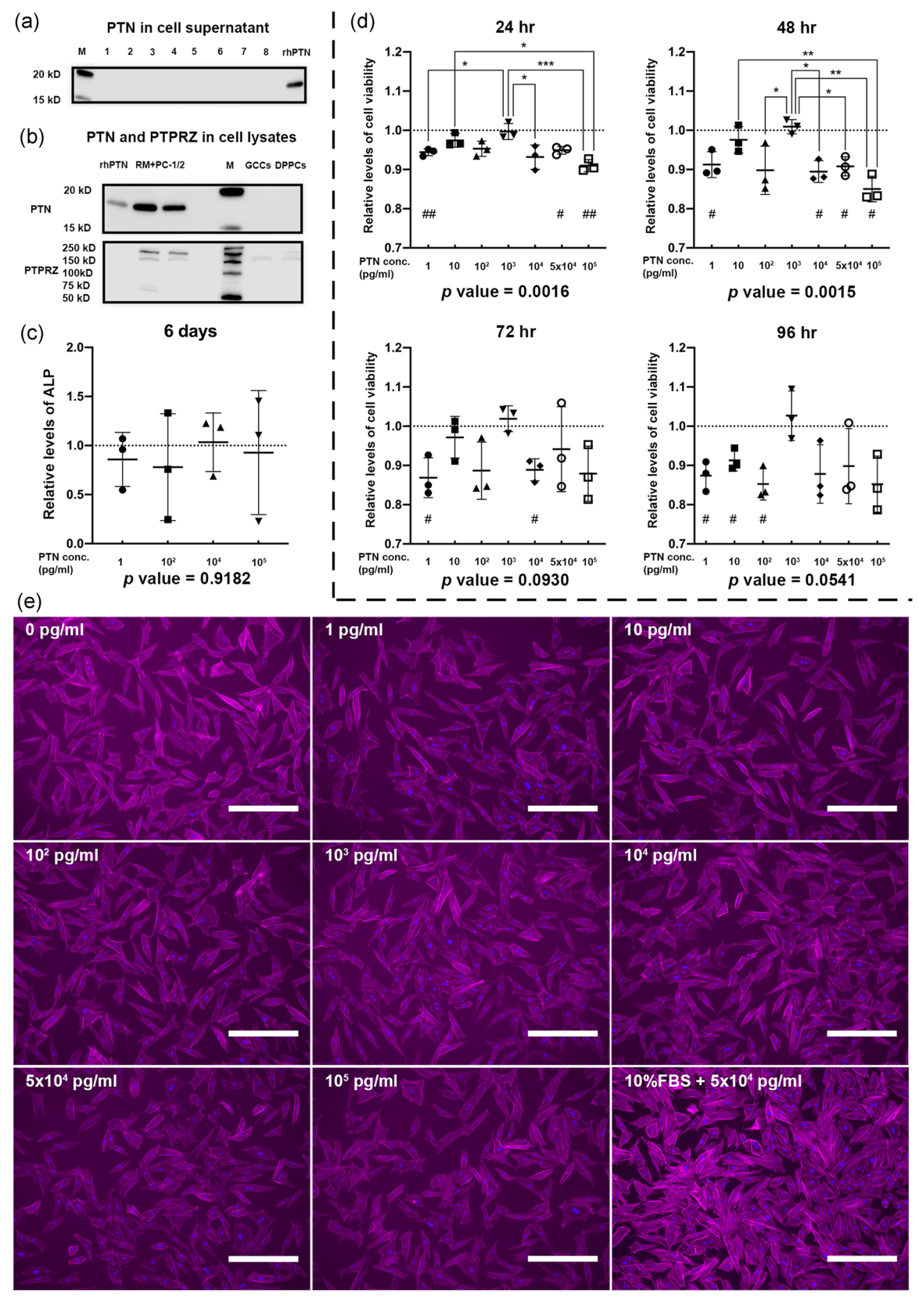


FIGURE 12 (See caption on next page)

Pleiotrophin mRNA expression level

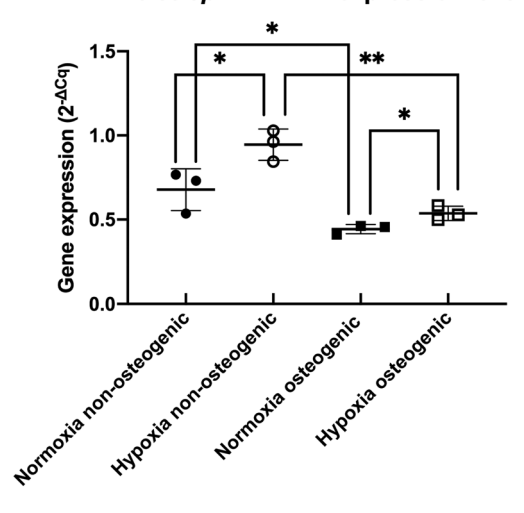


FIGURE 13 Gene expression levels of *pleiotrophin* as detected by quantitative reverse transcriptase real-time polymerase chain reaction (qRT²-PCR). Unpaired t tests were used. *p < .05, **p < .01. Data are presented as the mean value \pm standard deviation (n = 3). qRT²-PCR; normoxia or hypoxia nonosteogenic medium (with reduced serum) under normoxic or hypoxic culture; normoxia or hypoxia osteogenic medium (with reduced serum) under normoxic or hypoxic culture. mRNA, messenger RNA

inactivation, and the downstream processes such as the ALK-NPM fusion and the regulation of processes critical to rapid antler regeneration.

The NOTCH2 receptor has mainly been documented for its interactions with MDK rather than PTN (Xu et al., 2014), and activation by MDK has been reported to induce cell plasticity and motility in epithelial-mesenchymal transitioning and tumorigenesis (Gungor et al., 2011; Huang et al., 2008). Within the antler GC, positive staining around blood vessels for NOTCH2 was only faintly detected and the expression was not as widespread as for MDK. A similar expression pattern between MDK and NOTCH2 was, however, observed within the PC layer. The strongest positive signal for NOTCH2 was found within the hypertrophic chondrocytes.

Interestingly, it was the PTN ligand rather than MDK which was highly expressed in the cartilage layer. This co-localisation between PTN and NOTCH2 indicates their potential interaction, as has previously been found during ocular development (Cui & Lwigale, 2019) and haematopoietic stem cell expansion (Himburg et al., 2010). A role for NOTCH2 and PTN in cartilage maturation is novel and warrants further investigation.

ITGAV/ITGB3, which form a dimer, were detected separately in this study. They have previously been reported to function as receptors for PTN, inducing endothelial cell migration through PTPRZ (Mikelis et al., 2009). Within the antler, both integrins were only detected around blood vessels, consistent with a proangiogenic role. It was noted that their expression pattern in the blood vessels was almost identical to MDK. This suggests that MDK may potentially interacted with ITGAV/ITGB3 and other angiogenic molecules such as VEGF during rapid angiogenesis in the antler (Clark et al., 2006).

PTPRZ was identified as the critical receptor between PTN and its downstream effects within the GC. The detection of PTPRZ and PTN was then extended into four antler tissues from the different regenerative stages. PTPRZ has three main splice variants including two transmembrane isoforms PTPRZ-A and PTPRZ-B, and the secretory isoform PTPRZ-S. These isoforms are known to be regulated in different ways during development (Nishiwaki et al., 1998). In this study, the anti-PTPRZ antibody was raised against the sequence Leu32 to Glu189 in the N terminus of PTPRZ. In the western blot, the strongly stained upper bands (Figure 2b) were most likely extracellular fragments of PTPRZ-B (Z_B-ECF) and the lower bands Z-ECF70, a common domain in the three isoforms (Chow et al., 2008; Fujikawa et al., 2017). The Z_B-ECF was mainly found in the active antler stem cell tissues, indicating that PTPRZ-B could be the dominant PTPRZ isoform functioning in rapid antler regeneration. The extracellular domain of PTPRZ-B contributes to receptor binding and functions associated with cell adhesion and migration (Bourgonje et al., 2014). CTNNB1 is a known downstream cell adhesion molecule activated through dimerisation of the PTN/PTPRZ complex (Meng et al., 2000). Tyrosine-phosphorylated CTNNB1 is also correlated with cadherin-mediated cell adhesion (Balsamo et al., 1996).

FIGURE 12 Proliferation and osteogenic differentiation of deer antler stem cells. (a) The western blot analysis of pleiotrophin (PTN) in the deer antler stem cell supernatants. Sample numbers 1-4: Culture media from growth centre cells (GCCs). Numbers 1 and 3 were from normal media at 7 and 21 days, and Numbers 2 and 4 were from osteogenic media at 7 and 21 days. Sample numbers 5-8: Culture media from dormant pedicle periosteum cells. Numbers 5 and 7 were from normal media at 7 and 21 days, and Numbers 6 and 8 were from osteogenic media at 7 and 21 days. Fifty nanograms recombinant human PTN (rhPTN) was used as a positive control. (b) The western blot analysis of the expression levels of PTN and PTPRZ in the deer antler stem cell lysates. Two tissue lysates from reserve mesenchymal and precartilage layers (RM + PC-1/ 2) in the growth centre and 50 ng rhPTN were used as positive controls. (c) Osteogenic differentiation detection of GCCs at 6 days. All cell lines were cultured with 100-ng/ml BMP-2 and PTN concentrations at 1, 10², 10⁴, or 10⁵ pg/ml as indicated for 6 days. Data are presented as the mean value ± standard deviation. The dotted line denotes control cells without PTN. One-way ANOVA with post hoc Tukey HSD test was performed, and the statistical significance of one-way ANOVA is presented. (d) Cell viability of GCCs cultured in 1% FBS under PTN concentrations of 1, 10, 10^2 , 10^3 , 10^4 , 5×10^4 , or 10^5 pg/ml at 24, 48, 72, and 96 h. Data are presented as the mean value \pm standard deviation. The dotted line denotes control cells cultured in 1% FBS without PTN. One-way ANOVA with post hoc Tukey HSD analysis was performed, with significance shown with an asterisk. A one-sample t test was used to compare PTN treated and control cells, with significance shown with a hashtag. (e) F-actin staining of GCCs under different PTN concentrations shown in (d) at 96 h. All cells were grown in 1% FBS, unless otherwise indicated. Red indicates F-actin staining and blue indicates DAPI staining. Scale bar = 400 μm. ANOVA, analysis of variance; DAPI, 4',6diamidino-2-phenylindole; FBS, fetal bovine serum; HSD, honestly significant difference; M, marker; PTPRZ, protein tyrosine phosphatase receptor type Z. */#p < .05, **/#p < .01, ***p < .001

The constitutive expression of PTN dramatically disrupts CTNNB1mediated adhesion and increases cell migration (Meng et al., 2000; Xia et al., 2019). The expression pattern of CTNNB1 in different antler regeneration stages has been reported, which is consistent with PTN and PTPRZ expression (Dong et al., 2020), that is, the active stem cells have the highest expression levels, the dormant stem cells the lowest and the post-active stem cells have a higher expression level than the dormant stem cells, but without significance. The expression levels of PTN, PTPRZ, and CTNNB1, therefore, reflected the stem cell activation status. Taken together, the PTN-PTPRZ-CTNNB1 signalling axis may be involved in regulating cell adhesion and migration during endochondral bone formation in the antler, especially given that CTNNB1 is an essential part of Wnt signalling and stem cell renewal (Rao & Kuhl, 2010; J. Wang & Wynshaw-Boris, 2004). Further research is required to investigate the interaction between PTN and PTPRZ and CTNNB1 as well as the phosphorylation status of CTNNB1 within the GC.

In vitro studies revealed that cells harvested from both dormant and active antler stem cell niches, and cultured in osteogenic media had the potential to become osteoblasts, one of the main cell types in the growing antler. The detection for PTN in cultured cell lysates and supernatants indicated that no PTN was expressed from antler stem cells in vitro. In addition, only low levels of PTPRZ ($Z_B\text{-ECF}$) were found in cell lysates. This result was surprising, considering the very high levels of PTN and PTPRZ in vivo in the active antler stem cells. The dormant antler stem cells did not produce PTN either in vivo or in vitro. Exogenous PTN was then added to investigate its function in the cultured active antler stem cells. The results showed

that exogenous PTN did not contribute to osteogenesis, but it may maintain cell stemness in vitro. This is consistent with PTN's critical role in haematopoietic stem cell maintenance (Himburg et al., 2018). The lack of PTN expression may be explained by the recent finding that both HIF- 1α and HIF- 2α have been identified, using label-free proteomics, as the most upstream regulators within the active antler stem cells, suggesting that the active stem cell niche is, in fact, hypoxic during rapid antler regeneration (Dong et al., 2020). In other systems, hypoxia results in the increased expression of PTN and PTPRZ (Antoine et al., 2005; V. Wang et al., 2005, 2010; Y. Wang et al., 2014). The high expression levels of PTN and PTPRZ in vivo may, therefore, reflect the presence of a hypoxic niche within the GC. The hypoxic culture for GCCs in vitro showed that there was a significant, but mild, induction for PTN mRNA expression as compared with normoxic culture; however, high quantities of PTN were produced under both conditions. The normoxic incubation in vitro may, thus, have caused some change to the stem cell niche and a reduction in PTN gene expression. PTN, however, cannot be detected at the protein level using western blot. The reason is still unknown, but it could be due to the fact that either PTN was positively charged and was thus lost, or it degraded soon after secretion. Hypoxia in vitro, therefore, has a role in inducing PTN gene expression, but it does not appear to be critical.

In conclusion, our study revealed the potential functions of PTN in antler stem cells in vivo and in vitro. The PTN/PTPRZ complex may activate downstream pathways including NPM-ALK and CTNNB1, and regulate cell behaviour during the rapid antler regeneration (Figure 14). NOTCH2 may also bind with PTN, inducing bone

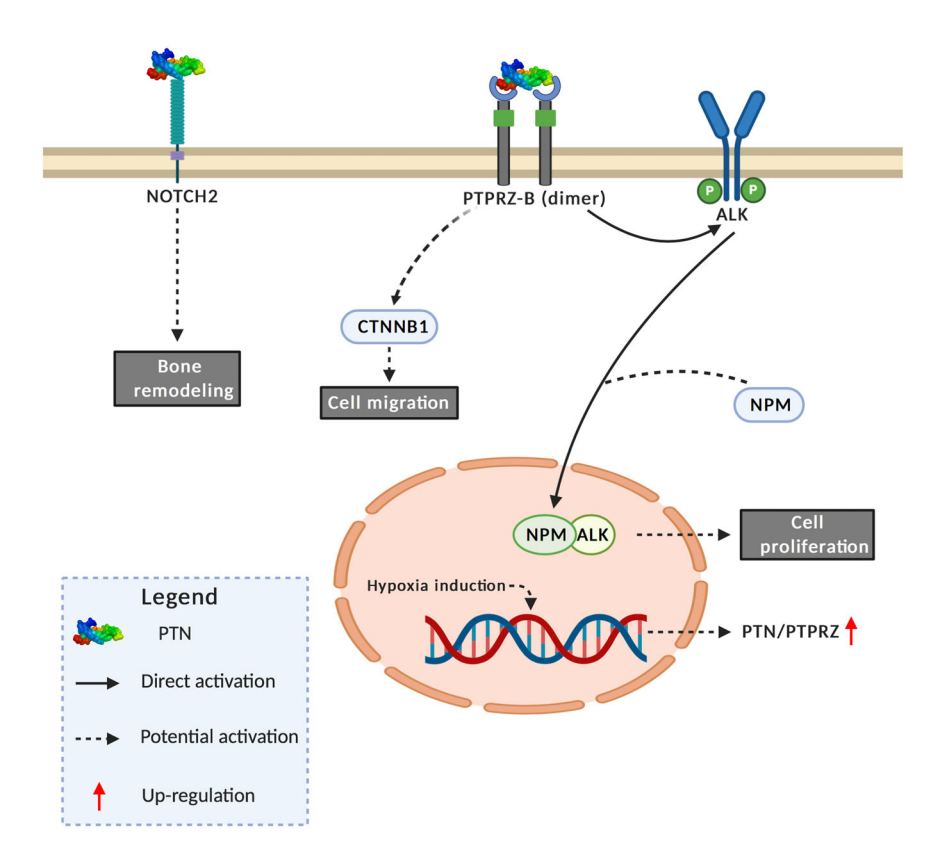


FIGURE 14 A schematic representation of the hypothetical mechanism shows potential functions of PTN during antler regeneration. The diagram was created with BioRender (https://biorender.com). ALK, anaplastic lymphoma kinase; NPM, nucleophosmin; PTN, pleiotrophin; PTPRZ, protein tyrosine phosphatase receptor type Z

remodelling. PTN may have an effect on the maintenance of stemness rather than differentiation under normoxic in vitro culture of antler stem cells.

ACKNOWLEDGEMENTS

This study was supported by Velvet Antler Research New Zealand and the University of Otago. The authors would like to thank Dr. Trudy Milne for kindly reading the manuscript. They would also like to thank Dr. Michael Pankhurst for kindly providing the facilities for conducting the hypoxia experiments.

CONFLICT OF INTERESTS

The authors declare that there are no conflict of interests.

AUTHOR CONTRIBUTIONS

Dawn Coates, Zhen Dong, and Chunyi Li designed the research. Dawn Coates, Chunyi Li, and Zhen Dong collected tissues. Zhen Dong and Dawn Coates performed the research. Zhen Dong and Dawn Coates analysed data. Zhen Dong wrote the manuscript. Dawn Coates helped in data interpretation and presentation, and critically revised the manuscript. Chunyi Li reviewed the manuscript.

DATA AVAILABILITY STATEMENT

The data that support the findings of this study are available from the corresponding author upon reasonable request.

ORCID

Zhen Dong https://orcid.org/0000-0002-3480-3421
Chunyi Li https://orcid.org/0000-0001-7275-4440
Dawn Coates https://orcid.org/0000-0003-4242-6846

REFERENCES

- Altschul, S. F., Madden, T. L., Schaffer, A. A., Zhang, J., Zhang, Z., Miller, W., & Lipman, D. J. (1997). Gapped BLAST and PSI-BLAST: A new generation of protein database search programs. *Nucleic Acids Research*, 25(17), 3389–3402. https://doi.org/10.1093/nar/25. 17.3389
- Antoine, M., Tag, C. G., Wirz, W., Borkham-Kamphorst, E., Sawitza, I., Gressner, A. M., & Kiefer, P. (2005). Upregulation of pleiotrophin expression in rat hepatic stellate cells by PDGF and hypoxia: Implications for its role in experimental biliary liver fibrogenesis. Biochemical and Biophysical Research Communications, 337(4), 1153–1164. https://doi.org/10.1016/j.bbrc.2005.09.173
- Balsamo, J., Leung, T., Ernst, H., Zanin, M. K., Hoffman, S., & Lilien, J. (1996). Regulated binding of PTP1B-like phosphatase to N-cadherin: Control of cadherin-mediated adhesion by dephosphorylation of beta-catenin. *Journal of Cell Biology*, 134(3), 801–813. https://doi.org/10.1083/jcb.134.3.801
- Bancroft, J. D., & Stevens, A. (1991). Theory and practice of histological techniques. World Publishing Corporation.
- Bischof, D., Pulford, K., Mason, D. Y., & Morris, S. W. (1997). Role of the nucleophosmin (NPM) portion of the non-Hodgkin's lymphoma-associated NPM-anaplastic lymphoma kinase fusion protein in oncogenesis. *Molecular and Cellular Biology*, 17(4), 2312–2325. https://doi.org/10.1128/mcb.17.4.2312
- Bouderlique, T., Henault, E., Lebouvier, A., Frescaline, G., Bierling, P., Rouard, H., Courty, J., Albanese, P., & Chevallier, N. (2014).

- Pleiotrophin commits human bone marrow mesenchymal stromal cells towards hypertrophy during chondrogenesis. *PLoS One*, *9*(2), e88287. https://doi.org/10.1371/journal.pone.0088287
- Bourgonje, A. M., Navis, A. C., Schepens, J. T. G., Verrijp, K., Hovestad, L., Hilhorst, R., Harroch, S., Wesseling, P., Leenders, W. P. J., & Hendriks, W. J. A. J. (2014). Intracellular and extracellular domains of protein tyrosine phosphatase PTPRZ-B differentially regulate glioma cell growth and motility. *Oncotarget*, 5(18), 8690–8702. https://doi.org/10.18632/oncotarget.2366
- Chiarle, R., Voena, C., Ambrogio, C., Piva, R., & Inghirami, G. (2008). The anaplastic lymphoma kinase in the pathogenesis of cancer. *Nature Reviews: Cancer*, 8(1), 11–23. https://doi.org/10.1038/nrc2291
- Choudhuri, R., Zhang, H. T., Donnini, S., Ziche, M., & Bicknell, R. (1997). An angiogenic role for the neurokines midkine and pleiotrophin in tumorigenesis. *Cancer Research*, *57*(9), 1814–1819. https://www.ncbi.nlm.nih.gov/pubmed/9135027
- Chow, J. P., Fujikawa, A., Shimizu, H., Suzuki, R., & Noda, M. (2008). Metalloproteinase- and gamma-secretase-mediated cleavage of protein-tyrosine phosphatase receptor type Z. *Journal of Biological Chemistry*, 283(45), 30879–30889. https://doi.org/10.1074/jbc. M802976200
- Clark, D. E., Lord, E. A., & Suttie, J. M. (2006). Expression of VEGF and pleiotrophin in deer antler. Anatomical Record. Part A: Discoveries in Molecular, Cellular, and Evolutionary Biology, 288(12), 1281–1293. https://doi.org/10.1002/ar.a.20393
- Cui, R., & Lwigale, P. (2019). Expression of the heparin-binding growth factors midkine and pleiotrophin during ocular development. *Gene Expression Patterns*, 32, 28–37. https://doi.org/10.1016/j.gep.2019. 02.001
- Deuel, T. F. (2013). Anaplastic lymphoma kinase: "Ligand Independent Activation" mediated by the PTN/RPTPbeta/zeta signaling pathway. Biochimica et Biophysica Acta, 1834(10), 2219–2223. https://doi.org/ 10.1016/j.bbapap.2013.06.004
- Dong, Z., Haines, S., & Coates, D. (2020). Proteomic profiling of stem cell tissues during regeneration of deer antler: A model of mammalian organ regeneration. *Journal of Proteome Research*, 19(4), 1760–1775. https://doi.org/10.1021/acs.jproteome.0c00026
- Fleming, R. J. (1998). Structural conservation of Notch receptors and ligands. Seminars in Cell and Developmental Biology, 9(6), 599–607. https://doi.org/10.1006/scdb.1998.0260
- Fujikawa, A., Chow, J. P. H., Matsumoto, M., Suzuki, R., Kuboyama, K., Yamamoto, N., & Noda, M. (2017). Identification of novel splicing variants of protein tyrosine phosphatase receptor type Z. *Journal of Biochemistry*, 162(5), 381–390. https://doi.org/10.1093/jb/mvx042
- Fukada, M., Fujikawa, A., Chow, J. P., Ikematsu, S., Sakuma, S., & Noda, M. (2006). Protein tyrosine phosphatase receptor type Z is inactivated by ligand-induced oligomerization. FEBS Letters, 580(17), 4051–4056. https://doi.org/10.1016/j.febslet.2006.06.041
- Goss, R. (1983). Deer antlers, regeneration, evolution and function. Academic Press.
- Gungor, C., Zander, H., Effenberger, K. E., Vashist, Y. K., Kalinina, T., Izbicki, J. R., Yekebas, E., & Bockhorn, M. (2011). Notch signaling activated by replication stress-induced expression of midkine drives epithelial-mesenchymal transition and chemoresistance in pancreatic cancer. *Cancer Research*, 71(14), 5009–5019. https:// doi.org/10.1158/0008-5472.CAN-11-0036
- Hampton, B. S., Marshak, D. R., & Burgess, W. H. (1992). Structural and functional characterization of full-length heparin-binding growth associated molecule. *Molecular Biology of the Cell*, 3(1), 85–93. https://doi.org/10.1091/mbc.3.1.85
- Herradon, G., Ezquerra, L., Nguyen, T., Silos-Santiago, I., & Deuel, T. F. (2005). Midkine regulates pleiotrophin organ-specific gene expression: Evidence for transcriptional regulation and functional redundancy within the pleiotrophin/midkine developmental gene

- family. Biochemical and Biophysical Research Communications, 333(3), 714–721. https://doi.org/10.1016/j.bbrc.2005.05.160
- Himburg, H. A., Harris, J. R., Ito, T., Daher, P., Russell, J. L., Quarmyne, M., Doan, P. L., Helms, K., Nakamura, M., Fixsen, E., Herradon, G., Reya, T., Chao, N. J., Harroch, S., & Chute, J. P. (2012). Pleiotrophin regulates the retention and self-renewal of hematopoietic stem cells in the bone marrow vascular niche. *Cell Reports*, 2(4), 964–975. https://doi.org/10.1016/j.celrep.2012.09.002
- Himburg, H. A., Muramoto, G. G., Daher, P., Meadows, S. K., Russell, J. L., Doan, P., Chi, J. T., Salter, A. B., Lento, W. E., Reya, T., Chao, N. J., & Chute, J. P. (2010). Pleiotrophin regulates the expansion and regeneration of hematopoietic stem cells. *Nature Medicine*, 16(4), 475–482. https://doi.org/10.1038/nm.2119
- Himburg, H. A., Termini, C. M., Schlussel, L., Kan, J., Li, M., Zhao, L., Fang, T., Sasine, J. P., Chang, V. Y., & Chute, J. P. (2018). Distinct bone marrow sources of pleiotrophin control hematopoietic stem cell maintenance and regeneration. *Cell Stem Cell*, 23(3), 370–381. e375. https://doi.org/10.1016/j.stem.2018.07.003
- Himburg, H. A., Yan, X., Doan, P. L., Quarmyne, M., Micewicz, E., McBride, W., Chao, N. J., Slamon, D. J., & Chute, J. P. (2014). Pleiotrophin mediates hematopoietic regeneration via activation of RAS. Journal of Clinical Investigation, 124(11), 4753–4758. https://doi.org/10.1172/JCI76838
- Huang, Y., Hoque, M. O., Wu, F., Trink, B., Sidransky, D., & Ratovitski, E. A. (2008). Midkine induces epithelial-mesenchymal transition through Notch2/Jak2-Stat3 signaling in human keratinocytes. *Cell Cycle*, 7(11), 1613–1622. https://doi.org/10.4161/cc.7.11.5952
- Hynes, R. O. (2002). Integrins: Bidirectional, allosteric signaling machines. Cell, 110(6), 673–687. https://doi.org/10.1016/S0092-8674(02) 00971-6
- Kadomatsu, K., Kishida, S., & Tsubota, S. (2013). The heparin-binding growth factor midkine: The biological activities and candidate receptors. *Journal of Biochemistry*, 153(6), 511–521. https://doi.org/ 10.1093/jb/mvt035
- Kaplan, F., Comber, J., Sladek, R., Hudson, T. J., Muglia, L. J., Macrae, T., Gagnon, S., Asada, M., Brewer, J. A., & Sweezey, N. B. (2003). The growth factor midkine is modulated by both glucocorticoid and retinoid in fetal lung development. American Journal of Respiratory Cell and Molecular Biology, 28(1), 33–41. https://doi.org/10.1165/ rcmb.2002-0047oc
- Ker, D. F. E., Wang, D., Sharma, R., Zhang, B., Passarelli, B., Neff, N., Li, C., Maloney, W., Quake, S., & Yang, Y. P. (2018). Identifying deer antler uhrf1 proliferation and s100a10 mineralization genes using comparative RNA-seq. Stem Cell Research & Therapy, 9(1), 292. https://doi.org/10.1186/s13287-018-1027-6
- Kishida, S., Mu, P., Miyakawa, S., Fujiwara, M., Abe, T., Sakamoto, K., Onishi, A., Nakamura, Y., & Kadomatsu, K. (2013). Midkine promotes neuroblastoma through Notch2 signaling. *Cancer Research*, 73(4), 1318–1327. https://doi.org/10.1158/0008-5472.CAN-12-3070
- Lamprou, M., Kaspiris, A., Panagiotopoulos, E., Giannoudis, P. V., & Papadimitriou, E. (2014). The role of pleiotrophin in bone repair. *Injury*, 45(12), 1816–1823. https://doi.org/10.1016/j.injury.2014. 10.013
- Levy, J. B., Canoll, P. D., Silvennoinen, O., Barnea, G., Morse, B., Honegger, A. M., Huang, J. T., Cannizzaro, L. A., Park, S. H., & Druck, T. (1993). The cloning of a receptor-type protein tyrosine phosphatase expressed in the central nervous system. *Journal of Biological Chemistry*, 268(14), 10573–10581. https://www.ncbi.nlm. nih.gov/pubmed/8387522
- Li, C. (2012). Deer antler regeneration: A stem cell-based epimorphic process. Birth Defects Research. Part C, Embryo Today: Reviews, 96(1), 51–62. https://doi.org/10.1002/bdrc.21000
- Li, C., Clark, D. E., Lord, E. A., Stanton, J. A., & Suttie, J. M. (2002). Sampling technique to discriminate the different tissue layers of

- growing antler tips for gene discovery. *Anatomical Record*, 268(2), 125–130. https://doi.org/10.1002/ar.10120
- Li, C., Mackintosh, C. G., Martin, S. K., & Clark, D. E. (2007). Identification of key tissue type for antler regeneration through pedicle periosteum deletion. *Cell and Tissue Research*, 328(1), 65–75. https://doi.org/10.1007/s00441-006-0333-y
- Li, C., & Suttie, J. M. (2003). Tissue collection methods for antler research. *European Journal of Morphology*, 41(1), 23–30. https://doi.org/10.1076/ejom.41.1.23.28106
- Li, C., Yang, F., & Sheppard, A. (2009). Adult stem cells and mammalian epimorphic regeneration-insights from studying annual renewal of deer antlers. *Current stem cell research* & therapy, 4(3), 237–251. https://doi.org/10.2174/157488809789057446
- Li, Y. S., Milner, P., Chauhan, A., Watson, M., Hoffman, R., Kodner, C., Milbrandt, J., & Deuel, T. (1990). Cloning and expression of a developmentally regulated protein that induces mitogenic and neurite outgrowth activity. *Science*, 250(4988), 1690–1694. https://doi.org/10.1126/science.2270483
- Li, Y. S., Hoffman, R. M., Le Beau, M. M., Espinosa, R., 3rd, Jenkins, N. A., Gilbert, D. J., & Deuel, T. F. (1992). Characterization of the human pleiotrophin gene. Promoter region and chromosomal localization. *Journal of Biological Chemistry*, 267(36), 26011–26016. https://www. ncbi.nlm.nih.gov/pubmed/1464612
- Meng, K., Rodriguez-Pena, A., Dimitrov, T., Chen, W., Yamin, M., Noda, M., & Deuel, T. F. (2000). Pleiotrophin signals increased tyrosine phosphorylation of beta beta-catenin through inactivation of the intrinsic catalytic activity of the receptor-type protein tyrosine phosphatase beta/zeta. Proceedings of the National Academy of Sciences of the United States of America, 97(6), 2603–2608. https://doi.org/10.1073/pnas.020487997
- Merenmies, J., & Rauvala, H. (1990). Molecular cloning of the 18-kDa growth-associated protein of developing brain. *Journal of Biological Chemistry*, 265(28), 16721–16724. https://www.ncbi.nlm.nih.gov/pubmed/2170351
- Mikelis, C., Sfaelou, E., Koutsioumpa, M., Kieffer, N., & Papadimitriou, E. (2009). Integrin alpha(v)beta(3) is a pleiotrophin receptor required for pleiotrophin-induced endothelial cell migration through receptor protein tyrosine phosphatase beta/zeta. FASEB Journal, 23(5), 1459–1469. https://doi.org/10.1096/fj.08-117564
- Minoo, P., & Wang, H. Y. (2012). ALK-immunoreactive neoplasms. International Journal of Clinical and Experimental Pathology, 5(5), 397–410. https://www.ncbi.nlm.nih.gov/pubmed/22808292
- Muramatsu, H., Zou, P., Kurosawa, N., Ichihara-Tanaka, K., Maruyama, K., Inoh, K., Sakai, T., Chen, L., Sato, M., & Muramatsu, T. (2006). Female infertility in mice deficient in midkine and pleiotrophin, which form a distinct family of growth factors. *Genes to Cells*, 11(12), 1405–1417. https://doi.org/10.1111/j.1365-2443.2006.01028.x
- Muramatsu, T. (2014). Structure and function of midkine as the basis of its pharmacological effects. *British Journal of Pharmacology*, 171(4), 814–826. https://doi.org/10.1111/bph.12353
- Nishiwaki, T., Maeda, N., & Noda, M. (1998). Characterization and developmental regulation of proteoglycan-type protein tyrosine phosphatase zeta/RPTPbeta isoforms. *Journal of Biochemistry*, 123(3), 458–467. https://doi.org/10.1093/oxfordjournals.jbchem. a021959
- Papadimitriou, E., Pantazaka, E., Castana, P., Tsalios, T., Polyzos, A., & Beis, D. (2016). Pleiotrophin and its receptor protein tyrosine phosphatase beta/zeta as regulators of angiogenesis and cancer. *Biochimica et Biophysica Acta*, 1866(2), 252–265. https://doi.org/10.1016/j.bbcan.2016.09.007
- Perez-Pinera, P., Zhang, W., Chang, Y., Vega, J. A., & Deuel, T. F. (2007).

 Anaplastic lymphoma kinase is activated through the pleiotrophin/
 receptor protein-tyrosine phosphatase beta/zeta signaling pathway:

 An alternative mechanism of receptor tyrosine kinase activation.

- Journal of Biological Chemistry, 282(39), 28683-28690. https://doi.org/10.1074/jbc.M704505200
- Powers, C., Aigner, A., Stoica, G. E., McDonnell, K., & Wellstein, A. (2002).
 Pleiotrophin signaling through anaplastic lymphoma kinase is rate-limiting for glioblastoma growth. *Journal of Biological Chemistry*, 277(16), 14153–14158. https://doi.org/10.1074/jbc.M112354200
- Rao, T. P., & Kuhl, M. (2010). An updated overview on Wnt signaling pathways: A prelude for more. Circulation Research, 106(12), 1798–1806. https://doi.org/10.1161/CIRCRESAHA.110.219840
- Rauvala, H., & Pihlaskari, R. (1987). Isolation and some characteristics of an adhesive factor of brain that enhances neurite outgrowth in central neurons. *Journal of Biological Chemistry*, 262(34), 16625–16635. https://www.ncbi.nlm.nih.gov/pubmed/3680268
- Sakurai, H., Bush, K. T., & Nigam, S. K. (2001). Identification of pleiotrophin as a mesenchymal factor involved in ureteric bud branching morphogenesis. *Development*, 128(17), 3283–3293. https://www.ncbi.nlm.nih.gov/pubmed/11546745
- Seifert, A. W., & Voss, S. R. (2013). Revisiting the relationship between regenerative ability and aging. *BMC Biology*, 11, 2. https://doi.org/10. 1186/1741-7007-11-2
- Sone, M., Muramatsu, H., Muramatsu, T., & Nakashima, T. (2011). Morphological observation of the stria vascularis in midkine and pleiotrophin knockout mice. *Auris Nasus Larynx*, 38(1), 41–45. https://doi.org/10.1016/j.anl.2010.05.005
- Stoica, G. E., Kuo, A., Aigner, A., Sunitha, I., Souttou, B., Malerczyk, C., Caughey, D. J., Wen, D., Karavanov, A., Riegel, A. T., & Wellstein, A. (2001). Identification of anaplastic lymphoma kinase as a receptor for the growth factor pleiotrophin. *Journal of Biological Chemistry*, 276(20), 16772–16779. https://doi.org/10.1074/jbc.M010660200
- Wang, D., Ba, H., Li, C., Zhao, Q., & Li, C. (2018). Proteomic analysis of plasma membrane proteins of antler stem cells using label-free LC(-) MS/MS. International Journal of Molecular Sciences, 19(11), 3477. https://doi.org/10.3390/ijms19113477
- Wang, D., Berg, D., Ba, H., Sun, H., Wang, Z., & Li, C. (2019). Deer antler stem cells are a novel type of cells that sustain full regeneration of a mammalian organ-deer antler. *Cell Death & Disease*, 10(6), 443. https://doi.org/10.1038/s41419-019-1686-y
- Wang, J., & Wynshaw-Boris, A. (2004). The canonical Wnt pathway in early mammalian embryogenesis and stem cell maintenance/ differentiation. Current Opinion in Genetics and Development, 14(5), 533–539. https://doi.org/10.1016/j.gde.2004.07.013
- Wang, V., Davis, D. A., Haque, M., Huang, L. E., & Yarchoan, R. (2005). Differential gene up-regulation by hypoxia-inducible factor-1alpha

- and hypoxia-inducible factor-2alpha in HEK293T cells. *Cancer Research*, 65(8), 3299–3306. https://doi.org/10.1158/0008-5472. CAN-04-4130
- Wang, V., Davis, D. A., Veeranna, R. P., Haque, M., & Yarchoan, R. (2010). Characterization of the activation of protein tyrosine phosphatase, receptor-type, Z polypeptide 1 (PTPRZ1) by hypoxia inducible factor-2 alpha. PLoS One, 5(3), e9641. https://doi.org/10.1371/journal.pone.0009641
- Wang, Y., Qiu, B., Liu, J., Zhu, W. G., & Zhu, S. (2014). Cocaine- and amphetamine-regulated transcript facilitates the neurite outgrowth in cortical neurons after oxygen and glucose deprivation through PTN-dependent pathway. *Neuroscience*, 277, 103–110. https://doi. org/10.1016/j.neuroscience.2014.06.064
- Wellstein, A. (2012). ALK receptor activation, ligands and therapeutic targeting in glioblastoma and in other cancers. *Frontiers in Oncology*, 2, 192. https://doi.org/10.3389/fonc.2012.00192
- Xia, Z., Ouyang, D., Li, Q., Li, M., Zou, Q., Li, L., Yi, W., & Zhou, E. (2019). The expression, functions, interactions and prognostic values of PTPRZ1: A review and bioinformatic analysis. *Journal of Cancer*, 10(7), 1663–1674. https://doi.org/10.7150/jca.28231
- Xu, C., Zhu, S., Wu, M., Han, W., & Yu, Y. (2014). Functional receptors and intracellular signal pathways of midkine (MK) and pleiotrophin (PTN). Biological and Pharmaceutical Bulletin, 37(4), 511–520. https://doi.org/10.1248/bpb.b13-00845
- Zou, P., Muramatsu, H., Sone, M., Hayashi, H., Nakashima, T., & Muramatsu, T. (2006). Mice doubly deficient in the midkine and pleiotrophin genes exhibit deficits in the expression of beta-tectorin gene and in auditory response. *Laboratory Investigation*, 86(7), 645–653. https://doi.org/10.1038/labinvest.3700428

SUPPORTING INFORMATION

Additional Supporting Information may be found online in the supporting information tab for this article.

How to cite this article: Dong Z, Li C, Coates D. PTN-PTPRZ signalling is involved in deer antler stem cell regulation during tissue regeneration. *J Cell Physiol.* 2020;1–18.

https://doi.org/10.1002/jcp.30115